
ArCHer: Training Language Model Agents via Hierarchical Multi-Turn RL

Yifei Zhou¹, Andrea Zanette¹, Jiayi Pan¹, Sergey Levine¹ and Aviral Kumar²

¹University of California, Berkeley, ²Google DeepMind

Abstract: A broad use case of large language models (LLMs) is in goal-directed decision-making tasks (or “agent” tasks), where an LLM needs to not just generate probable completions for a given prompt, but rather make intelligent decisions over an extended period of multi-turn interaction to accomplish a task (e.g., when interacting with the web, using software tools, or engaging in customer support). Reinforcement learning (RL) provides a general paradigm to address such agent tasks, but current RL methods for LLMs largely focus on single-turn reward maximization. By construction, single-turn RL methods of today cannot actually train LLMs to intelligently seek and incorporate information over multiple turns, perform credit assignment, or reason about their past actions – all of which are critical in agent tasks. This raises the question: how can we design effective and efficient multi-turn RL algorithms for LLMs? In this paper, we propose an algorithmic framework for developing multi-turn RL algorithms for fine-tuning LLMs, that preserves the flexibility of existing single-turn RL methods for LLMs (e.g., proximal policy optimization), while accommodating multiple turns, long horizons, and delayed rewards effectively. To do this, our framework adopts a hierarchical RL approach and runs two RL algorithms in parallel: a high-level off-policy RL algorithm that trains a value function to aggregate reward over utterances, and a low-level RL algorithm that utilizes this high-level value function (in place of a reward model used in single-turn RL) to train a token-by-token policy within each utterance or turn. This hierarchical approach prescribed by our framework, **Actor-Critic Framework with a Hierarchical Structure (ArCHer)**, can also give rise to a number of other RL approaches. Empirically, we find that ArCHer significantly improves efficiency and performance on multi-turn tasks, attaining sample efficiency of about **100x** over existing on-policy methods, while also benefitting favorably from scaling up model capacity (upto the 7 billion scale that we could test on in our experiments). Project page can be found in <https://yifeizhou02.github.io/archer.io/> and code can be found in <https://github.com/YifeiZhou02/ArCHer>.

1. Introduction

Owing to their generalist knowledge, large language models (LLMs) have a tremendous potential to address a wide variety of decision-making or “agent” problems that can be expressed in text or natural language, from writing code (Yang et al., 2023a; Li et al., 2022; Lin et al., 2018), navigating the web (Zhou et al., 2023a; Yao et al., 2023a), and using tools (Schick et al., 2023), all the way to interacting with humans (Ghosal et al., 2022; Verma et al., 2022; Jaques et al., 2020). In order to succeed in these domains, an LLM needs to make a *sequence* of intelligent decisions over multiple turns of interaction instead of generating the most *probable* text completion at each step.

Despite these multi-turn agent problems, most methods for eliciting goal-directed behavior from LLMs often rely on myopic objectives that either attempt to mimic successful demonstrations at each step (Zeng et al., 2023; Chen et al., 2023), or otherwise optimize for single-turn preferences (Touvron et al., 2023; Ouyang et al., 2022; Bai et al., 2022). Policies trained via single-turn approaches often fail to perform effective credit assignment (e.g., they fail to identify good actions that may lead to long-term future performance despite appearing suboptimal at a given step) and do not endow policies with information-seeking behavior, which is important in agent problems (e.g., when dealing with a new tool). Therefore, in this paper, we consider the problem of building multi-turn RL approaches that are able to directly maximize long-term objective of interest (e.g., customer satisfaction at the end of a multi-turn conversation with an LLM assistant), formulated via a scalar reward function.

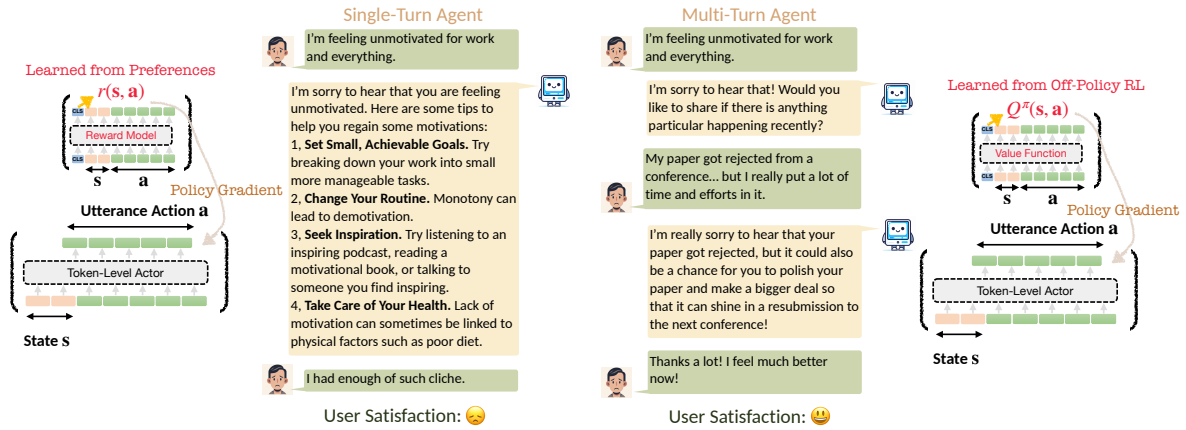


Figure 1: Single-turn RL vs multi-turn RL for LLMs (ours). In particular, the single-turn RL agent seeks to resolve the request within a single turn and hence ends up providing as much information as possible in its response. On the contrary, the multi-turn RL agent can execute information-gathering actions and address requests in a targeted manner over turns. While current single-turn RL methods for LLMs abstractly use some form of policy gradients computed using a reward model to train the LLM policy, the method proposed in our paper extends this paradigm to the multi-turn setting by now replacing the reward model with a learned value function, which is trained with off-policy reinforcement learning.

Unlike single-step RL (Touvron et al., 2023; Ouyang et al., 2022; Bai et al., 2022), training LLMs via multi-turn RL presents a number of unique challenges. First of all, multi-turn RL would require online interaction with external sources such as humans or web servers, which can be slow and expensive. Due to this, on-policy methods such as PPO (Schulman et al., 2017) quickly become impractical owing to their inability to reuse data from past interaction. While off-policy fully offline methods circumvent this problem, these methods present other challenges: since the number of tokens increase with multiple turns (often substantially so, due to the bias of LLMs towards producing long responses), token-level methods (Snell et al., 2023; Jaques et al., 2020) that consider individual tokens as actions need to now propagate reward signal over extremely long horizons. This results in extremely slow learning speeds over long horizons for token-level algorithms. For example, token-level ILQL (Snell et al., 2023) takes more than 10 days to converge on a task in our experiments, while filtered behavior cloning takes less than a day. In principle, to address long horizon issues, one can treat the entire utterance for each turn as an action (Verma et al., 2022; Jang et al., 2022), but this comes at the cost of introducing an enormous, variable-size action space, presenting a challenge for off-policy methods based on temporal-difference (TD) learning that require maximization over the action at each time step. This necessitates a multi-turn RL framework that can attain a sweet spot in terms of the aforementioned challenges.

In this paper, we devise a framework for building multi-turn RL algorithms that attains this kind of a sweet spot. Our key insight is that a **hierarchical approach** for RL with language models that addresses the challenges with both on-policy and off-policy RL approaches as outlined above. Specifically, our framework prescribes an off-policy temporal difference learning method for training an utterance-level value function at the high level, and any on-policy policy gradient algorithm for optimizing the token generation at each turn of the interaction at the low level, treating the high-level value function as the terminal reward for that turn. Unlike on-policy methods, this allows for sample reuse and faster convergence, while avoiding Bellman backups over individual tokens or maximization over enormous action spaces, as the high-level critic is trained at a coarser time-scale, on tokens produced by the actor. In addition, it also directly inherits implementation details from existing token-level RL algorithms developed for single-turn RL with preferences, for training the policy. This way we are able to obtain the best of both utterance-based and token-based, and off-policy and on-policy approaches for training LLMs.

Our main contribution is a framework for developing hierarchical RL approaches for LLMs, that we call: Actor-Critic framework with a **Hierarchical Structure** (or **ArCHer** in short). We study several concrete algorithmic instantiations derived from the ArCHer framework by conducting experiments on a range of language “agent” tasks with active data collection (i.e., the “online” setting). We find that algorithms derived from ArCHer are 100x more sample efficient than on-policy methods such as PPO, and converge to a better performance than off-policy methods. Moreover, our methods are easy to build on existing single-turn RL methods and scale to different transformer architectures and more parameters (we show effectiveness of our approach up to the 7 billion scale), directly enabling plug-and-play choices of RL algorithms and models.

2. Related Work

Single-turn reinforcement learning for LLMs. Most prior works that use RL for LLMs have focused on decision-making problems where the language model must produce a single decision, with no further steps of interaction with an external environment (e.g., the “single-turn” preference optimization setting (Casper et al., 2023; Christiano et al., 2023; Ziegler et al., 2019)). Typical algorithms used for this sort of single-turn RL include policy-gradient methods such as PPO (Ouyang et al., 2022; OpenAI et al., 2023; Ramamurthy et al., 2023), A2C (Glaese et al., 2022), offline optimization methods such as DPO (Rafailov et al., 2023), and filtered supervised learning approaches (Yuan et al., 2023; Korbak et al., 2023; Gulcehre et al., 2023). Despite promising results, there remain many important agent problems that cannot be solved in a single-turn setting. Many of these problems require the agent to explicitly take the steps to gather information before making a decision, such as asking for personalized preferences before making a travel plan (Hong et al., 2023) or initially attempting to read the help manual of the shell in a linux terminal, before carrying out the requested tasks (Liu et al., 2023). Single-step approaches cannot learn such nuanced strategies as they attempt to solve the problem within a single step, necessitating multi-turn RL methods for training LLMs.

Training language agents without RL. Motivated by few-shot learning and reasoning abilities of LLMs, prior works also utilize LLMs for sequential decision-making via prompt engineering. For example, ReAct (Yao et al., 2023b) and Reflexion (Shinn et al., 2023) prompt the LLM to “think” and analyze past failures before executing the next action. Voyager (Wang et al., 2023) prompts the LLM agent to develop and refine a curriculum and action library based on environment input. However, without updating the parameters of the LLM, the effectiveness of these methods is inherently limited by the intrinsic capabilities obtained from pre-training (Zeng et al., 2023; Chen et al., 2023). Even state-of-the-art models such as GPT-4 with in-context learning can perform very sub-optimally in out-of-distribution settings (Liu et al., 2023; Yang et al., 2023b) without updating the model. To improve over pre-trained capabilities, another line of work finetunes LLMs with successful trajectories (generated manually or by rolling out a strong pre-trained LLM) (Schick et al., 2023; Zeng et al., 2023; Chen et al., 2023). However, manual labels and tool call annotations are expensive to obtain. Moreover, it would be prohibitively expensive for automated approaches to stumble upon successful rollouts will as the task horizon increases (Liu et al., 2023; Abdulhai et al., 2023). Therefore, in this paper, we sidestep these problems by directly maximizing the objective of interest via RL. **Multi-turn RL for LLMs.** While many prior works directly use off-the-shelf policy-gradient methods, such as PPO (Schulman et al., 2017; Szot et al., 2023; Yao et al., 2023a) and REINFORCE (Sutton et al., 1999; Williams, 2004; Ranzato et al., 2015; Wu and Hu, 2018; Paulus et al., 2017) to train LMs, these methods can become sample inefficient in multi-step settings that require interaction with an external environment (Verma et al., 2022; Jang et al., 2022). To address such sample complexity issues, off-policy and offline value-based methods learn from existing static data (Snell et al., 2023; Jaques et al., 2020; Verma et al., 2022; Jang et al., 2022). However, existing off-policy methods for multi-turn language tasks either (1) consider a single token as an action (i.e., “token-level”) (Snell et al., 2023;

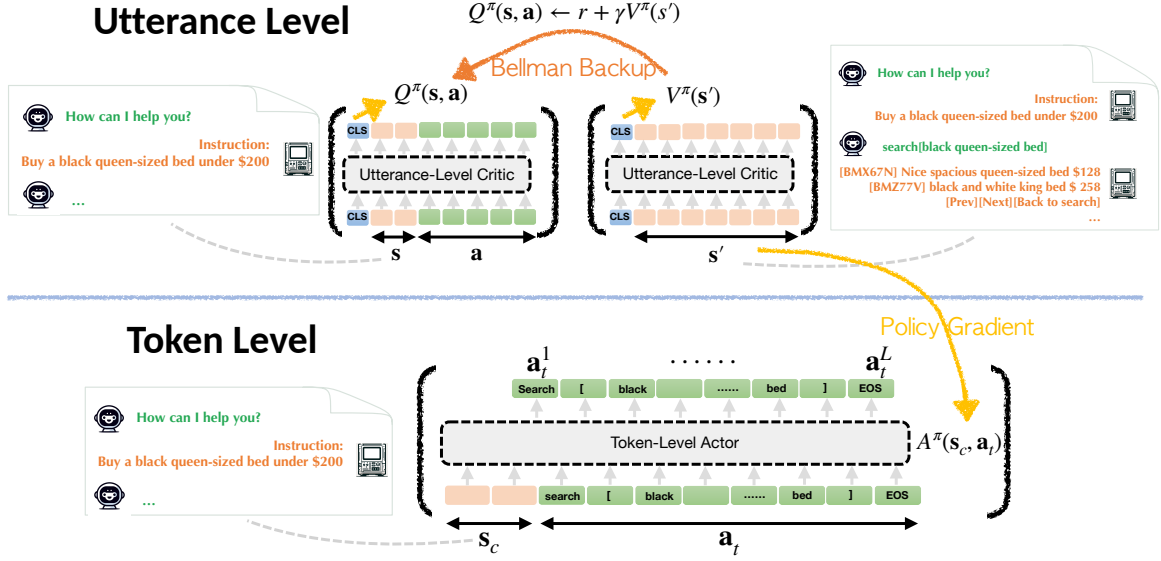


Figure 2: Schematic of the practical instantiation of Actor-Critic Framework with a Hierarchical Structure (ArCHer). Our algorithm operates both at the utterance level and the token level. At the utterance level, our algorithm learns a Q-function, via Bellman bootstrapping with TD errors. At the token level, the policy is learned by maximizing the advantage function induced by the utterance-level Q-function using a policy gradient approach, where this advantage estimate is provided as a reward at the end of the sequence of tokens appearing within the utterance.

Jaques et al., 2020) and must deal with long horizons, or (2) consider an utterance as a single action, but utilize multiple candidate utterances from a frozen pre-trained LLM for maximization in the Bellman backup (Verma et al., 2022; Jang et al., 2022), reducing the pace of policy improvement, as we also find in our experiments. Our approach will address both of these limitations.

3. Actor-Critic Framework with a Hierarchical Structure (ArCHer)

Existing RL methods that consider an individual token as an action suffer from very long horizons with multiple turns. Utterance-level RL methods avoid this challenge, but now they must tractably maximize over a coherent set of tokens within an utterance. To address these issues, we will develop a class of hierarchical RL methods, ArCHer, that bypass these challenges by running two RL algorithms, in parallel. We start by describing how multi-turn language generation can be posed as a hierarchical Markov decision process (MDP), followed by building RL methods in this hierarchical MDP.

3.1. Language Generation as a Hierarchical MDP

In order to derive effective multi-turn RL algorithms, we will now present a novel formulation of language generation as acting in a hierarchical MDP. Our construction defines a *high-level* MDP, and a *low-level* MDP embedded inside the high-level MDP. For both MDPs, states are a variable-length sequence of tokens. For the high-level MDP, an action is defined as a sequence of tokens. An action in the low-level MDP is a single token, such that executing a sequence of actions in the low-level MDP corresponds to a single action in the high-level MDP. Formally, each state s_t in the high-level MDP consists of an interaction history between the LLM and the external environment, and each action a_t in this MDP is a variable-length sequence of tokens. The low-level MDP models the generation of the high-level action produced by the agent *within* a single high-level action, where each low-level action a_t^h is an individual token (i.e., the h -th token in the t -th high-level action). A state in this low-level MDP is obtained by concatenating a high-level state s_c consisting of the interaction history until this turn and $a_t^{1:h-1}$, the history of individual action tokens produced within the current turn before step

h . The next state is obtained by concatenating the current action to this token history. Figure 2 shows a visualization of our notations for the hierarchical MDP.

Policy optimization in the high-level MDP aims to maximize task reward, whereas a policy in the low-level MDP attempts to find a sequence of up to L tokens $a_t^{1:L}$ that maximizes reward equal to the value function of the high-level MDP $Q^\pi(s, a_t^{1:L})$, provided at the end of the low-level rollout. A rollout in the low-level MDP ends as soon as the policy ends up choosing to produce an “EOS” token.

A concrete and natural instantiation of this hierarchical framework in the context of multi-turn interactions is when each turn or an “utterance” corresponds to a single time step in the high-level MDP, and each token within a turn is an action in the low-level MDP. In other words, this construction chooses to use the utterance-level MDP (Figure 2) at the high level and the token-level MDP at the low level. For example, in the context of a web agent, the state would be the interaction of web pages visited so far and a high-level action would be an utterance, e.g., “search[queen-sized bed, black]”. A candidate reward function would be +1 if the correct item can be bought and 0 otherwise. The dynamics would involve the web engine reacting to an action. Each token of an utterance (e.g., “search[queen-sized bed, black]”) would be an individual action in the embedded token-level MDP, for example, an action would be individual tokens “search”, “[”, “queen”.

3.2. Preliminaries: Reinforcement Learning Definitions

In order to describe the details of our framework, we first provide a few standard RL definitions. The Q function of a policy π is the expected long-term return obtained by executing a certain action at the current step, followed by executing π thereafter: $Q^\pi(s_h, a_h) = \mathbb{E}_\pi [\sum_{t=0}^{\infty} \gamma^t r(s_{h+t}, a_{h+t})]$. The value function $V^\pi(s_h)$ is given by taking an expectation of the Q-value, $Q^\pi(s_h, a_h)$, under actions a_h sampled from the policy π . The advantage $A^\pi(s_h, a_h)$ of a state-action pair is the difference between its Q-value and the value of the state under the policy: $A^\pi(s_h, a_h) = Q^\pi(s_h, a_h) - V^\pi(s_h)$. We will denote the value function in the low-level MDP as $\tilde{V}(s_c, a_h^{1:i-1})$.

3.3. RL Algorithms in the Hierarchical Language MDP

The proposed hierarchical MDP provides flexibility in designing multi-turn RL algorithms: we could use any choice of RL algorithm for either the high or the low level. That said, note that only the high level requires interaction with a (non-differentiable) environment, while the low level optimizes against the high-level value function, and therefore trains entirely “in silico,” without any interaction with an environment. Therefore, the requirements on these methods are different: the high-level algorithm should be highly sample efficient, while the low-level algorithm should be easy to optimize. A particularly convenient choice is to use TD learning at the high level, while using on-policy methods (Ouyang et al., 2022; Bai et al., 2022) at the low level.

3.4. A Practical Instantiation of ArCHer for Sample-Efficient Online RL

For deriving a concrete practical algorithm, we will utilize the natural hierarchical MDP induced in multi-turn language interaction: the utterance-level MDP at the high level and the embedded token-level MDP at low level, as discussed at the end of Section 3.1. In this setting, our approach would train an utterance-level critic with TD backups and a token-level policy with policy gradients.

High-level utterance critic. Following the practice in prior RL algorithms (Snell et al., 2023), we train two LLM models at the high-level, one to represent the utterance-level Q-function $Q_\theta^\pi(s, a)$, and one to represent the utterance-level value function, $V_\psi^\pi(s)$. The Q-model is trained on Bellman targets computed from a delayed copy of the value-model. And the value model, in turn, is trained to approximate the expected value of the Q-model on token sequences (i.e., utterances) obtained by sampling autoregressively from the low-level policy, π_ϕ . Due to the off-policy nature of this training

process, we store and train on data from all previous online interactions $\mathcal{D} = \{s_i, a_i, r_i, s'_i\}_{i=1}^N$. The objective for training the Q-model and the value-model are formally given by:

$$J_Q(\theta) = \mathbb{E}_{s,a,r,s' \sim \mathcal{D}} [(Q_\theta(s, a) - r - \gamma V_{\bar{\psi}}(s'))^2]. \quad (\text{Bellman consistency between } Q_\theta \text{ and } V_{\bar{\psi}}) \quad (1)$$

$$J_V(\psi) = \mathbb{E}_{s \sim \mathcal{D}} \left[\mathbb{E}_{a \sim \pi_\phi(\cdot|s)} [(V_\psi(s) - Q_{\bar{\theta}}(s, a))^2] \right]. \quad (\text{Train } V_\psi \text{ to approximate } \mathbb{E}_{a \sim \pi_\phi(\cdot|s)} [Q_{\bar{\theta}}(s, a)]) \quad (2)$$

We estimate Equation 2 by sampling a batch of n observations $\{s_i\}_{i=1}^n$, followed by auto-regressively sampling token sequences from the actor $\{a_t^L\}_{i=1}^n$. The delayed target models $Q_{\bar{\theta}}$ and $V_{\bar{\psi}}$ are updated towards their current counterparts with Polyak averaging (Haarnoja et al., 2018).

Low-level token actor. At the low-level, we train the token-level actor $\pi_\phi(\cdot|s_c, a_t^{1:h})$ via an on-policy policy gradient approach to find a sequence of tokens that maximizes the prediction of the Q-model. To reduce variance, we use advantage values derived from the Q-model as the terminal reward. This subroutine for training the actor generalizes single-turn RL methods from RLHF, except that the terminal reward is now an estimate of the multi-turn advantage instead of a reward model. Concretely, we update the token-level policy with the policy gradient computed via REINFORCE (Williams, 2004):

$$J_\phi(\pi) = \mathbb{E}_{s_c \sim \mathcal{D}, a_t^{1:L} \sim \pi(\cdot|s_c)} \left[\sum_{i=1}^L A(s_c, a_t^{1:L}) \log \pi_\phi(a_t^i | s_c, a_t^{1:i-1}) \right]. \quad (3)$$

3.5. Other Practical ArCHer Algorithms

The instantiation of ArCHer described in Section 3.4 is simple and ready-to-use, but the flexibility of the ArCHer framework also enables it to incorporate other components that prior works found to be successful. We describe two variants in the two paragraphs to follow. The first improves the sample efficiency while interacting with the external environment and the second enables ArCHer to learn entirely from a dataset of pre-collected experience.

Improvements to token-level policy gradient. In applications where the horizon of the token-level MDP is long (i.e. each utterance has many tokens), despite the use of advantage values (instead of Q-model predictions directly), the REINFORCE estimator corresponding to Equation 3 can struggle to improve the policy due to a high variance in token-level reward (Schulman et al., 2015). This variance can be reduced by introducing a baseline value function, $\tilde{V}_\eta(\tilde{\pi})$ parameterized by η , in the token-level MDP. For simplicity, we opt to train this token-level baseline via supervised regression onto Monte-Carlo return estimates (with a discount factor of 1.0) in the token-level MDP as shown in Equation 4, though Bellman backups can also be employed in the low-level MDP to estimate it:

$$J_\eta(\tilde{V}) = \mathbb{E}_{s_c \sim \mathcal{D}, a_t^{1:L} \sim \pi(\cdot|s_c)} \left[\sum_{i=1}^L \left(A(s_c, a_t^{1:L}) - \tilde{V}_\eta(s_c, a_t^{1:i-1}) \right)^2 \right]. \quad (4)$$

Incorporating this token-level baseline, the new objective for the actor given by Equation 5:

$$J_\phi(\pi) = \mathbb{E}_{s_c \sim \mathcal{D}, a_t^{1:L} \sim \pi(\cdot|s_c)} \left[\sum_{i=1}^L \left(A(s_c, a_t^{1:L}) - \tilde{V}_\eta(s_c, a_t^{1:i-1}) \right) \cdot \log \pi_\phi(a_t^i | s_c, a_t^{1:i-1}) \right]. \quad (5)$$

Offline RL training with ArCHer. ArCHer can also learn from a dataset of pre-collected experience without any online interaction. A distinguishing aspect of the offline setting is that improving the policy normally results in selecting out-of-distribution actions (Kumar et al., 2019), whose Q values

are difficult to estimate accurately given only the offline dataset. As a result, directly optimizing the Q values, as in the online setting, often results in severe overestimation, divergence, and poor policy performance. This suggests that we need to adopt different objective functions in this offline setting. One concrete instantiation is to utilize the implicit Q-learning (IQL) (Kostrikov et al., 2021) algorithm for obtaining backup targets for the utterance-level critic restricted to in-support actions, and the AWR (Peng et al., 2019) algorithm for imposing a penalty on deviating far away from the data on the actor. While our offline RL experiments utilize these design choices, one could also utilize other techniques such as explicitly regularizing the critic’s predictions (Kumar et al., 2020) or imposing a behavioral cloning loss on the actor (Fujimoto and Gu, 2021).

The IQL loss aims to derive a version of the TD error that aims to inherit characteristics of the Bellman optimality operator but without performing an explicit maximization over the actions, by instead regressing Q -functions towards a higher expectile of possible target values at the next state. For a given expectile parameter $\tau \in [0.5, 1)$, the IQL loss is given by the following:

$$J_{\psi}^{\text{IQL}}(V) = \mathbb{E}_{s \sim \mathcal{D}} [\mathbb{E}_{a \sim \pi_{\phi}(\cdot|s)} [L_2^{\tau}(V_{\psi}(s) - Q_{\bar{\theta}}(s, a))]], \quad (6)$$

where $L_2^{\tau}(u) = |\tau - \mathbf{1}\{u < 0\}|u^2$. See the paper Kostrikov et al. (2021) for more details.

The policy extracted by AWR (Peng et al., 2019) trades off between searching for high-return policies and imitating the policy that generated the dataset, by minimizing the loss

$$J_{\phi}(\pi) = -\mathbb{E}_{(s_c, a_t^{1:L}) \sim \mathcal{D}} \left[\exp(\beta \cdot A(s_c, a_t^{1:L})) \cdot \sum_{i=1}^L \log \pi_{\phi}(a_t^i | s_c, a_t^{1:i-1}) \right]. \quad (7)$$

The tradeoff is controlled by a positive, user-defined scalar value β . Low values for β encourage imitating the policy that generated the dataset. Large values of β lead to more aggressive maximization of rewards, but potentially at the cost of stability (Peng et al., 2019).

3.6. Framework Summary and Practical Implementation Details

Pseudocode. The algorithms derived from the ArCHer framework so far are summarized in Algorithm 1. These algorithms can operate in either offline or online mode (Line 4), and can utilize a variety of objectives for training the utterance-level Q - and V -models (Lines 9-15) as well the token-level policy (Line 20). Optionally, a token-level baseline value function may also be utilized (Line 17).

Implementation details. In our main experiments, we use a GPT-2 (Radford et al., 2019) architecture for parameterizing the policy, and a RoBERTa-base model (Liu et al., 2019) with a linear layer on top of the embeddings corresponding to the “[CLS]” token for obtaining the critic’s predictions. To address the issue of overestimation of Q -values, we also employ the double Q-learning trick (van Hasselt et al., 2015) and train two copies of Q - and V -models, $\{Q_1, V_1\}$ and $\{Q_2, V_2\}$, independently. The advantage value is calculated by using a minimum over Q_1, Q_2 and V_1, V_2 .

To save computation and memory costs, Q_1, Q_2, V_1, V_2 share the same language model encoder backbone with separate MLP heads. The parameters of the token-level actor are independent from the critic. When utilized, the token-level value baseline is parameterized by a separate GPT2 architecture with a MLP layer on top of the hidden states for each token. Additional details and hyperparameters for our approach are provided in Appendix F.

4. Theoretical Analysis

We will present empirical results showing the effectiveness of ArCHer in Section 5, but in this section we will first highlight some theoretical and conceptual benefits of our hierarchical design. An important

Algorithm 1 ArCHer: Practical Framework

```

1: Initialize parameters  $\phi, \psi, \theta, \bar{\theta}$ , (Optionally)  $\eta$ 
2: Initialize replay buffer  $\mathcal{D}$  (optionally from an offline dataset).
3: for each iteration do
4:   ## Data Collection. ▷ [only online mode]
5:   for each environment step do
6:     Execute  $a_t \sim \pi_\phi(\cdot|s_t)$ , obtain the next state  $s_{t+1}$ , add to buffer  $\mathcal{D}$ .
7:   end for
8:   for each critic step do
9:     ## Update utterance-level Q and V functions by target function bootstrapping.
10:     $\theta \leftarrow \theta - \nabla J_\theta(Q)$  ▷ Equation 1
11:     $\psi \leftarrow \psi - \nabla J_\psi(V)$  ▷ Equation 2 or 6
12:    ## Update target Q and V functions.
13:     $\bar{\theta} \leftarrow (1 - \tau)\bar{\theta} + \tau\theta$ 
14:     $\bar{\psi} \leftarrow (1 - \tau)\bar{\psi} + \tau\psi$ 
15:   end for
16:   ## Update token-level baseline by MC regression.
17:   for each baseline step do
18:     $\eta \leftarrow \eta - \nabla J_\eta(\tilde{V})$  ▷ (Optionally), Equation 4
19:   end for
20:   ## Update token-level actor with utterance-level critic.
21:   for each actor step do
22:     $\phi \leftarrow \phi - \nabla J_\phi(\pi)$  ▷ Equation 3, 5, or 7
23:   end for
24: end for

```

difference between ArCHer and prior token-level RL algorithms such as ILQL (Snell et al., 2023) is the high-level critic. Thus, we aim to understand the impact of estimation errors in this high-level critic on the token-level policy in contrast with the impact of estimation errors in a token-level critic. While our proof techniques can be easily applied to general high-level and low-level MDPs, we focus on analyzing the specific contrast of utterance and token-level critics to be concrete.

Conditions for convergence. To start, we show that a hierarchical RL design prescribed by ArCHer requires substantially weaker conditions for algorithm convergence compared to off-policy token-level methods. These conditions pertain to **(1)** the capacity of the function class representing the critic (i.e., Bellman completeness (Song et al., 2023; Zhou et al., 2023b; Zanette, 2023; Xie et al., 2021)), and **(2)** the coverage of off-policy data as measured by the density ratio (Zhan et al., 2022; Foster et al., 2021), following the practice standard in RL theory. For **(1)**, we show in Lemma 1 that satisfying the Bellman completeness (Song et al., 2023; Zhou et al., 2023b; Zanette, 2023; Xie et al., 2021) condition imposes weaker requirements on the function class used to model the critic at the utterance-level (as is the case with ArCHer) as opposed to the token level. Intuitively, this is because a function class representing the token-level critic must exhibit flexibility to realize arbitrary functions at the next token, which would require higher capacity compared to a utterance-level critic that only needs to be able to realize arbitrary functions at the coarser time-scale of utterances.

For **(2)**, we show in Lemma 2 that the density ratio condition (Zhan et al., 2022; Foster et al., 2021) imposes identical requirements on the coverage of the offline data for token-level and utterance-level critic, despite a larger space of possible utterances (i.e., actions in the higher-level MDP). Intuitively, this is because the a given offline dataset induces the same trajectory distribution at both the utterance

and token levels. In other words, if a trajectory is covered by the offline data at the utterance level, it is also covered by the offline data at the token level, and vice versa.

Statistical error analysis with finite samples. With the convergence conditions discussed above, we are able to establish an analysis of the statistical error incurred in estimating the advantage estimates using the utterance-level and token-level critics. Intuitively, this means that an utterance-level critic provides a much more correct signal for improving the policy. We state the conclusions of the theorem below, and refer interested readers to Appendix G for formal definitions and proof.

Theorem 1 (Main Theorem; Informal). *For an utterance-level MDP with discount factor γ , where L is the maximum length of each utterance, suppose utterance-level Assumption 1 and 2 holds, let f be the final Q-function returned by fitted policy evaluation formalized in Algorithm 2 at the utterance level, f yields a suboptimality gap of*

$$\mathbb{E}_{s,a \sim d^\pi} \left[\left((\bar{f}(s,a) - \mathbb{E}_{a' \sim \pi(\cdot|s)}[\bar{f}(s,a)]) - A^\pi(s,a) \right)^2 \right] \leq \frac{1}{\gamma L^{1/2}} \mathcal{O} \left(\frac{1}{(1-\gamma)(1-\gamma^{1/L})L^{1/2}} (\epsilon_{stat} + \sqrt{\epsilon_{stat}}) \right).$$

For an equivalent token-level MDP with discount factor $\gamma^{1/L}$, suppose token-level Assumption 1 and 2 holds, let f be the final Q function returned by Fitted Policy Evaluation formalized in Algorithm 2 at the token level, f yields a suboptimality gap of

$$\mathbb{E}_{s,a \sim \tilde{d}^\pi} \left[\left((\bar{f}(s,a) - \mathbb{E}_{a' \sim \pi(\cdot|s)}[\bar{f}(s,a)]) - \tilde{A}^\pi(s,a) \right)^2 \right] \leq \mathcal{O} \left(\frac{1}{(1-\gamma)(1-\gamma^{1/L})L^{1/2}} (\epsilon_{stat} + \sqrt{\epsilon_{stat}}) \right),$$

where ϵ_{stat} is the statistical error, proportional to $N^{-1/2}$ (N is the number of utterance-level transitions).

Informally, Theorem 1 shows that the error in estimating advantages using the token-level critic is $\gamma\sqrt{L}$ larger than the the utterance-level critic (in the worst case), where L is the maximum number of tokens in each utterance, due to error accumulation. In practice, a common choice for γ is greater than 0.95 while L can be as large as 64 tokens, resulting in $\gamma L^{1/2} \gg 1$. Therefore, we have not only shown that a hierarchical design requires weaker conditions for convergence, but it also enjoys improved guarantees on the statistical error, resulting in a more accurate estimate of policy gradient for improving the policy in the worst case.

5. Experiments

The goal of our experiments is to evaluate the efficacy of hierarchical RL algorithms derived from ArCHer. Specifically, we aim to answer the following questions: (1) Is ArCHer able to achieve better sample complexity and performance than prior on-policy and off-policy RL methods for LLMs? (2) Does the TD-learning design for the utterance-level critic enable an effective use of off-policy data? (3) How does the performance of ArCHer scale with larger base models (such as Mistral 7B (Jiang et al., 2023))? (4) How do different practical algorithms derived from our ArCHer framework compare? To answer these questions, we will present an extensive empirical evaluation of ArCHer and several prior methods on a suite of environments encompassing natural language games, navigation problems posed in natural language, and interaction with the web.

5.1. Tasks and Environments

To stress-test the efficacy of ArCHer, we need environments and task setups that satisfy several desiderata. First, the chosen tasks must require strategic multi-step planning and reasoning under delayed rewards, and cannot be solved in one turn. We also want these tasks to require LLMs to generate coherent natural language and keep the task realistic.

Next, we want these tasks to be solvable by models of upto 7 billion parameter scale, which corresponds to the upper end of our computational budget. Finally, the chosen tasks should support fast and reliable evaluations, for reproducibility and benchmarking. Most existing LLM agent tasks such as those which require interacting with terminals, operating systems, and databases (Yang et al., 2023a; Liu et al., 2023) require larger base models (typically larger than 7B) for obtaining non-trivial success rates and can often be solved in a single step. This makes these tasks unfavorable for fast iteration within our compute budget. Other dialogue and tutoring tasks (Hong et al., 2023; Verma et al., 2022; Zhu et al., 2020; Lee et al., 2019; Budzianowski et al., 2018) require either costly user studies or evaluate using metrics that do not directly represent task performance, making them unfavorable for stress-testing our approach. Therefore, we utilize a different set of tasks for our evaluations.

Concretely, we consider the following tasks: **(1) Detective Game** (Hausknecht et al., 2019), an interactive text fiction game where the agent must generate a sequence of natural language actions (e.g., “take paper”, “eat apple”) based on environment feedback. A reward is given if the agent reaches some milestones towards finishing the game, where the end goal is to successfully find the murderer in a murder mystery; **(2) Twenty Questions** (Abdulhai et al., 2023), a dialogue task where the agent plays the role of a guesser trying to guess a hidden word from a list of 157 words within twenty yes/no questions. The oracle answers the questions with “Yes.”, “No.”, or “Invalid Question.” The oracle is simulated with a “flan-t5-small” (Chung et al., 2022) model trained with supervised fine-tuning on the dataset provided by Abdulhai et al. (2023). Upon guessing the correct word, the agent receives a reward of 0 and the environment terminates. Otherwise, a reward of -1 is provided at each time step. We also study a variation of this task with a list of only 10 possible underlying words, that we call **Twenty Questions Subset**. This variant challenges the algorithms to tailor a very specific strategy when there is a shortcut in the task; **(3) Guess My City** (Abdulhai et al., 2023), a similar multi-turn task where the agent attempts to guess the name of a hidden city from a list of 100 cities within twenty questions. A crucial difference between the Guess My City task and the Twenty Questions task is that the guesser is now allowed to ask any question and can observe free-form responses (which are not necessarily “Yes” or “No”); **(4) WebShop** (Yao et al., 2023a), a tool-use task where the agent is instructed to buy an item from a shopping server. A dense reward between 0 and 1 is provided based on the similarity of the item purchased and the item requested. See Appendix A for more details. These tasks require planning over long horizons, allow non-trivial success rates within the 7 billion parameter scale, and come equipped with reproducible and task-directed evaluation metrics.

5.2. Comparisons and Baseline Approaches

We compare our method to a number of alternative RL approaches. For token-level methods, we consider token-level PPO (Schulman et al., 2017) due to its state-of-the-art performance with LLMs (Ouyang et al., 2022; Ramamurthy et al., 2022). For each iteration, PPO collects new on-policy data by rolling out the current actor and uses these data to estimate the policy gradient. Perhaps most importantly, data collected by previous policies is simply discarded for later updates. We use the existing PPO implementation by Abdulhai et al. (2023). We also implemented a **token-level DQN** (Mnih et al., 2013) method, but were unable to get it to attain non-zero task performance. Neither did we find any prior work evaluating this method, and hence we omit it from our results.

We also considered a non-RL approach based on filtered behavioral cloning (BC), denoted as **Filtered BC**. As prior work (Abdulhai et al., 2023; Snell et al., 2023) shows, perhaps surprisingly, this simple baseline often attains competitive or better performance than RL approaches for LLMs, implying that outperforming filtered BC is a hallmark of proper functioning of the “RL component” in an approach. Our implementation of filtered BC maintains a fixed size buffer of recent rollouts and trains the actor with an imitation learning loss on the top 10% rollouts, as identified based on the total task reward.

For utterance-level methods, we compare with a state-of-the-art utterance-level RL method, CHAI (Verma

et al., 2022). CHAI was designed for offline RL specifically. To extend it to learn from online rollouts, we simply replace the pessimistic loss function (i.e., a conservative Q-learning (Kumar et al., 2020) loss) in this approach with a standard TD-learning loss function on data sampled from the off-policy replay buffer, identical to the one used in ArCHer. That said, the key difference is that CHAI utilizes a frozen actor obtained by behavioral cloning (or supervised fine-tuning) on the replay buffer, whereas ArCHer optimizes the actor as well. Each time when an action needs to be sampled, k utterances are sampled from the frozen actor. The utterance-level critic in CHAI ranks these k utterances and chooses the utterance with the highest Q value. A larger value of k would likely lead to better performance, but is also computationally expensive for this method. To obtain a sweet spot, we instantiate CHAI with $k = 5$ to effectively balance computational overhead and performance (**note that $k = 5$ already results in a runtime of about 4 times longer than our approach for this prior method**; going beyond would be prohibitive for our computational resources). Model architectures, learning rates, and other algorithm-agnostic details are kept identical between all prior methods and ArCHer (see Section 3.6).

Finally, akin to single-turn RL fine-tuning of LLMs, we initialize the token-level policy for all methods with a policy checkpoint obtained by running supervised instruction tuning on sub-optimal data for the task (see Appendix A for how this sub-optimal data is generated). Uniformly across all methods, this initialization enables effective exploration at the beginning of RL fine-tuning.

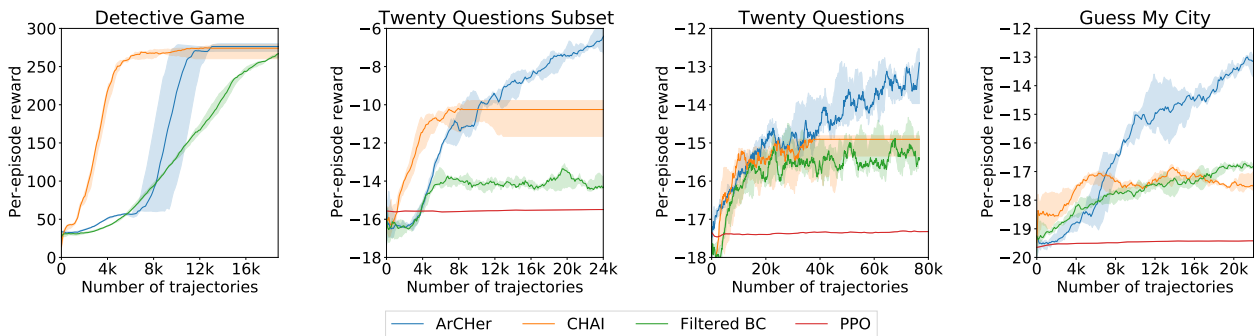


Figure 3: Online RL results comparing ArCHer and other approaches on four tasks. We plot the median performance of each method across three seeds. Observe that ArCHer steadily improves the policy, outperforming all other methods on three tasks and matching the best prior approach on the simple Detective Game task. While PPO appears to not be learning, by zooming into the learning curve in Figure 7, we find that PPO still gradually improves but at a very slow speed.

5.3. Results: Sample Efficiency in the Online Setting

Figure 3 and 4 show the comparison between ArCHer with other methods across the five tasks. We also provide some example rollouts of ArCHer for each environment in Appendix E. Overall, we found that ArCHer converges to a much better performance than all other prior methods on the four

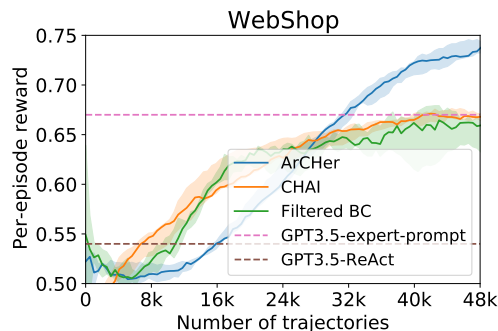


Figure 4: Webshop results. Observe that fine-tuning a GPT2 base model with ArCHer outperforms prior approaches, filtered BC and CHAI, and is the only approach to outperform GPT 3.5 equipped with several effective prompting strategies.

harder tasks that require identifying hidden information or present diverse initial states (i.e., Twenty Questions Subset, Twenty Questions, Guess My City, and WebShop). In fact, on WebShop, online RL training of GPT2 base model via ArCHer outperforms several effective prompting strategies (i.e., an expert-written prompt and ReAct (Yao et al., 2023b)) applied on top of GPT-3.5, a strong LLM.

First of all, we found that token-level PPO fails to achieve performance competitive with all other off-policy methods using the same amount of data. This is perhaps unsurprising, as PPO is an on-policy method, and therefore, cannot effectively reuse samples from past iterations. In particular, on the **Twenty Questions** task, we observed that PPO could only stably improve when provided with at least 1024 on-policy rollouts for each gradient step, likely because of high gradient variance. This observation corroborates the finding of Abdulhai et al. (2023), suggesting that online PPO is less practical for this task. Quantitatively, we find that while it takes more than 100k samples for PPO to attain an average return just higher than -17 (see Figure 7 in the appendix), ArCHer attains this reward value with fewer than 1000 samples, implying at least a **100x boost** in sample efficiency.

While filtered BC generally converges very quickly, the resulting policy often performs suboptimally and does not improve with more data in Figure 3. On the other hand, ArCHer enjoys steady policy improvement as it collects more samples. Finally, we observed that while CHAI improved at a faster than ArCHer initially, it often converged to a worse final performance. We suspect this is because the critic in CHAI is directly used to rerank samples from a frozen behavior policy, which only enables a narrow margin for policy improvement. On the contrary, ArCHer needs an initial learning phase to reduce critic estimation error, after which it can improve steadily.

5.4. Ablation Study: Importance of Off-Policy Data

In Figure 5 (b), we investigate the importance of off-policy data by varying the size of replay buffer on the **Guess My City** task. A smaller replay buffer means that updates rely on repeatedly sampling on-policy data. In our experiments, we observed that using a replay buffer containing only the most recent 48 rollouts resulted in unstable learning, likely due to overfitting on limited data, which has been observed in standard RL problems outside of LLMs (Nikishin et al., 2022). On the other hand, larger buffers are more stable. However, increasing the size of the buffer beyond a certain point is benign, resulting in no meaningful changes to performance. Overall, this means that making use of off-policy data can improve the stability and performance of practical methods.

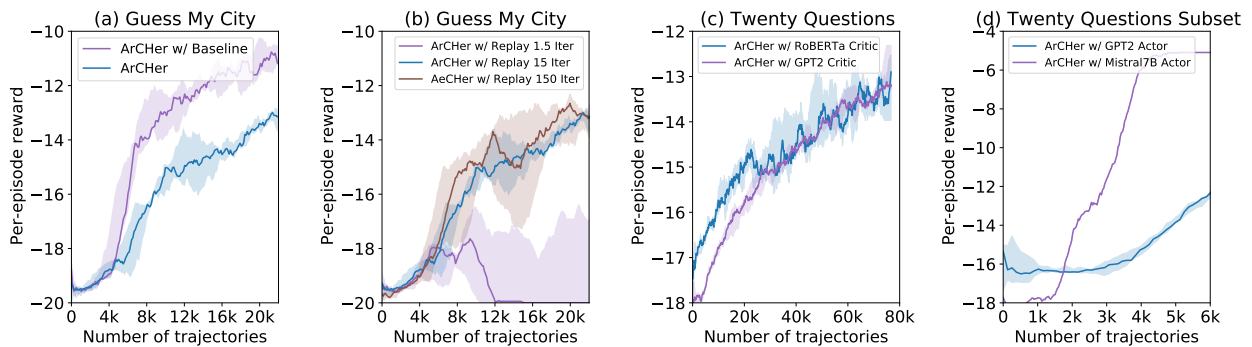


Figure 5: (a) Ablation study of the token-level baseline on Guess My City. (b) Ablation study of the importance of off-policy data by varying the size of the replay buffer on Guess My City. (c) Ablation study of changing the base model for critic from encoder-only RoBERTa to autoregressive decoder-only GPT2 on Twenty Questions. (d) Ablation study of scaling the base model for the actor from GPT2 to Mistral7B on Twenty Questions Subset.

5.5. Ablation Study: Alternate Base Models for the High-Level Critic in ArCHer

In Figure 5 (c), we carried out an ablation of changing the architecture for the critic model from an encoder-only RoBERTa (Liu et al., 2019) to an autoregressive decoder-only GPT2 (Radford et al.,

	Twenty Questions (Return)
ArCHer (IQL + AWR)	−14.1
ArCHer (IQL + REINFORCE)	−20
ArCHer (IQL + REINFORCE + BC)	−15.3
ArCHer (SARSA + AWR)	−14.5
Filtered BC	−15.4
BC	−16.8

Table 1: Variants of ArCHer in the offline RL setting. The performance of different approaches is evaluated by running 1280 trajectories across 5 random seeds for ArCHer and the Filtered BC approach. Observe that handling out-of-distribution actions by instantiating ArCHer with the IQL and AWR objectives works best in the offline setting.

2019), where we took the embedding of the last “[EOS]” token as the embedding of the utterances. Observe that although ArCHer w/ RoBERTa critic learns a bit faster in the beginning, learning curves for both of these critic models behave identically past a certain number of initial samples. Therefore, ArCHer can also use decoder-only transformer models, with no loss in performance.

5.6. Ablation Study: Scaling the Base Model from 100M to 7B Parameters

In Figure 5 (d), we replaced the 100 million parameter GPT-2 model used to represent the token-level actor in ArCHer with a 7 billion parameter Mistral model (Jiang et al., 2023). When using this 7B model, we did not need to apply supervised fine-tuning since the open-source checkpoint already attained non-trivial rewards on **Twenty Questions Subset** when evaluated zero-shot. Observe in Figure 5 (d), that ArCHer with this Mistral7B actor learns to solve the task much faster than ArCHer with a GPT2 Actor. This indicates that our ArCHer framework can scale well with LLMs with more parameters. More broadly, due to similarities between the token-level actor update in ArCHer and single-turn RL fine-tuning for LLMs in RLHF, we would expect performance to exhibit similar benefits from scaling the model size for the policy (Gao et al., 2023). This finding corroborates this hypothesis.

5.7. Alternate Practical Algorithms Derived from ArCHer

Online ArCHer with improved policy gradient estimators. In Figure 5 (a), we compare the performance of ArCHer with and without a token-level baseline on the **Guess My City** task (Equation 5). This task requires the utterances of the agent in each turn to be longer and more diverse than other tasks. Observe that incorporating this token-level baseline in ArCHer outperforms standard ArCHer by a large margin, supporting our hypothesis that the introduction of the token-level baseline can effectively reduce the variance of the vanilla policy gradient while updating the token-level actor (especially when the utterances are long and diverse). That said, this improvement requires paying an extra computational overhead associated with training \tilde{V}_η , which might not be necessary when each utterance is short. Overall, this study illustrates one of the central benefits of our hierarchical design: we can choose the best method for the higher and lower level based on their distinct requirements.

Offline ArCHer with IQL and AWR. We now present a preliminary study of ArCHer in the offline setting, when learning from a static dataset from past environment interactions. Due to computational constraints, we were not able to perform extensive comparisons with the state-of-the-art algorithms; rather, we investigated the effect of several design choices in order to investigate the effect of various design choices in the offline setting, including IQL and AWR losses described in Section 3.5. We also incorporate a baseline, **BC**, which performs (unfiltered) imitation learning on the offline dataset. Finally, we also ran filtered BC, which only imitates the best trajectories in the offline dataset.

In Table 1, we also evaluate several other design choices in the offline setting. Directly borrowing the

REINFORCE objective from the online setting (Equation 3) results in a quick collapse of performance due to the lack of any regularization to prevent out-of-distribution actions, as is well known in the offline RL problem setting outside of LLMs (Kumar et al., 2019). Combining Equation 3 with an imitation learning loss stabilizes learning and results in a performance improvement, but still underperforms advantage-weighted regression (AWR) (Peng et al., 2019). Finally, we replaced the IQL in-sample expectile backup with a SARSA backup, where the utterance present in the offline dataset at the next turn is used to compute the Bellman target, i.e., no implicit or explicit maximization over target values is utilized, and the value function is trained to represent the long-term Q-values of the data collection policy. Observe that this variant did not offer the same level of policy improvement as using IQL to train the critic in this setting. This highlights the importance of maximization over actions to calculate Bellman targets in the offline setting. Finally, we also find that instantiations of ArCHer that use IQL and SARSA in conjunction with AWR, both outperform the naïve BC and filtered BC, further highlighting the importance of dynamic programming to train the critic.

To summarize, our experiments show that ArCHer can be used to derive multi-turn RL methods that lead to substantial improvements to sample efficiency of LLM policy training, benefit from offline and off-policy experience as well as improvements to RL algorithms, and scale with model capacity.

6. Discussion and Conclusion

In this paper, we propose a novel Actor-Critic Framework with a Hierarchical Structure (ArCHer) for multi-turn LLM agent tasks. By running two RL algorithms simultaneously, one at the high level (i.e., utterances in our practical method) and one at the low level (i.e., tokens), ArCHer reduces task horizons while enjoying the ability to retain a compact token-level action space at the low level. These characteristics yield a more practical, efficient, and effective method for training LLMs to be effective decision-makers or agents. ArCHer is simple and extensible, and can be flexibly instantiated with a variety of components for both the high- and low-level methods. Empirically, we observed that ArCHer significantly outperforms prior RL methods for LLMs, on a range of online RL tasks and scales favorably with more capable base models and other design improvements.

Due to the computational constraints associated with running many trials of multiple RL algorithms and ArCHer instantiations, we had to conduct most of our experiments with a relatively small GPT-2 architecture. While our result with a Mistral7B base model demonstrates favorable scaling properties of our approach but rigorously evaluating our method with larger models (and on other benchmarks) is an important direction for future work. Our evaluations also focus entirely on tasks with computational rewards, and our method still requires a significant number of interactions (in the thousands), so an important future direction is to study how such methods can be made feasible to learn from live interactions with humans, when only about 100 interactions are available. We believe that model-based RL approaches could be quite promising here. Finally, deriving and evaluating novel practical algorithms from the hierarchical framework of ArCHer is also an interesting avenue for future work with the potential to greatly improve task performance.

Acknowledgements

We thank Seohong Park, Mitsuhiko Nakamoto, Joey Hong, Yi Su, and members of the RAIL lab at UC Berkeley for valuable feedback on a previous version of this paper. YZ and AZ thank Marwa Abdulhai, Isadora White, and Charlie Snell for help with debugging and setting up the LMRL benchmark. AK thanks Charlie Snell, George Tucker, and Young Geng for informative discussions and perspectives. This work is supported by NSF IIS-2246811 and ONR N00014-21-1-2838, TRC TPU credit donations from Google Cloud, and compute credit donations from the Center for AI Safety (CAIS). AZ is supported by a postdoctoral fellowship from the Simons Institute for the Theory of Computing.

Author Contributions

This work was done at UC Berkeley. Yifei Zhou led the project. He wrote the prototype of ArCHer, iterated on refining and improving it, implemented the baselines for online comparisons, and different ablation in the online experiments. He also took a lead in writing the paper. Andrea Zanette led the offline experiments of the project. He developed the offline variant of ArCHer with IQL and AWR, and helped editing the paper. Jiayi Pan set up the environment of webshop for our use and implemented prompting baselines. He also refactored the code and helped set up data distributed parallel training for ArCHer and baselines. Sergey Levine advised the project, provided inputs for prototyping the method, and helped editing the paper. Aviral Kumar proposed the project idea, advised the project, helped the prototyping of ArCHer, and substantially edited the paper.

References

- Marwa Abdulhai, Isadora White, Charlie Snell, Charles Sun, Joey Hong, Yuexiang Zhai, Kelvin Xu, and Sergey Levine. Lmrl gym: Benchmarks for multi-turn reinforcement learning with language models, 2023.
- Yuntao Bai, Andy Jones, Kamal Ndousse, Amanda Askell, Anna Chen, Nova DasSarma, Dawn Drain, Stanislav Fort, Deep Ganguli, Tom Henighan, Nicholas Joseph, Saurav Kadavath, Jackson Kernion, Tom Conerly, Sheer El-Showk, Nelson Elhage, Zac Hatfield-Dodds, Danny Hernandez, Tristan Hume, Scott Johnston, Shauna Kravec, Liane Lovitt, Neel Nanda, Catherine Olsson, Dario Amodei, Tom Brown, Jack Clark, Sam McCandlish, Chris Olah, Ben Mann, and Jared Kaplan. Training a helpful and harmless assistant with reinforcement learning from human feedback, 2022.
- Pawel Budzianowski, Tsung-Hsien Wen, Bo-Hsiang Tseng, Iñigo Casanueva, Stefan Ultes, Osman Ramadan, and Milica Gasic. Multiwoz - A large-scale multi-domain wizard-of-oz dataset for task-oriented dialogue modelling. *CoRR*, abs/1810.00278, 2018. URL <http://arxiv.org/abs/1810.00278>.
- Stephen Casper, Xander Davies, Claudia Shi, Thomas Krendl Gilbert, Jérémy Scheurer, Javier Rando, Rachel Freedman, Tomasz Korbak, David Lindner, Pedro Freire, Tony Wang, Samuel Marks, Charbel-Raphaël Segerie, Micah Carroll, Andi Peng, Phillip Christoffersen, Mehul Damani, Stewart Slocum, Usman Anwar, Anand Siththaranjan, Max Nadeau, Eric J. Michaud, Jacob Pfau, Dmitrii Krasheninnikov, Xin Chen, Lauro Langosco, Peter Hase, Erdem Biyık, Anca Dragan, David Krueger, Dorsa Sadigh, and Dylan Hadfield-Menell. Open problems and fundamental limitations of reinforcement learning from human feedback, 2023.
- Baian Chen, Chang Shu, Ehsan Shareghi, Nigel Collier, Karthik Narasimhan, and Shunyu Yao. Fireact: Toward language agent fine-tuning. *ArXiv*, abs/2310.05915, 2023. URL <https://api.semanticscholar.org/CorpusID:263829338>.
- Paul Christiano, Jan Leike, Tom B. Brown, Miljan Martic, Shane Legg, and Dario Amodei. Deep reinforcement learning from human preferences, 2023.
- Hyung Won Chung, Le Hou, Shayne Longpre, Barret Zoph, Yi Tay, William Fedus, Yunxuan Li, Xuezhi Wang, Mostafa Dehghani, Siddhartha Brahma, Albert Webson, Shixiang Shane Gu, Zhuyun Dai, Mirac Suzgun, Xinyun Chen, Aakanksha Chowdhery, Alex Castro-Ros, Marie Pellat, Kevin Robinson, Dasha Valter, Sharan Narang, Gaurav Mishra, Adams Yu, Vincent Zhao, Yanping Huang, Andrew Dai, Hongkun Yu, Slav Petrov, Ed H. Chi, Jeff Dean, Jacob Devlin, Adam Roberts, Denny Zhou, Quoc V. Le, and Jason Wei. Scaling instruction-finetuned language models, 2022.

- Dylan J. Foster, Akshay Krishnamurthy, David Simchi-Levi, and Yunzong Xu. Offline reinforcement learning: Fundamental barriers for value function approximation. *CoRR*, abs/2111.10919, 2021. URL <https://arxiv.org/abs/2111.10919>.
- Scott Fujimoto and Shixiang Shane Gu. A minimalist approach to offline reinforcement learning. In *Thirty-Fifth Conference on Neural Information Processing Systems*, 2021.
- Leo Gao, John Schulman, and Jacob Hilton. Scaling laws for reward model overoptimization. In *International Conference on Machine Learning*, pages 10835–10866. PMLR, 2023.
- Deepanway Ghosal, Siqi Shen, Navonil Majumder, Rada Mihalcea, and Soujanya Poria. Cicero: A dataset for contextualized commonsense inference in dialogues. In *Annual Meeting of the Association for Computational Linguistics*, 2022. URL <https://api.semanticscholar.org/CorpusID:247762111>.
- Amelia Glaese, Nat McAleese, Maja Trebacz, John Aslanides, Vlad Firoiu, Timo Ewalds, Maribeth Rauh, Laura Weidinger, Martin Chadwick, Phoebe Thacker, Lucy Campbell-Gillingham, Jonathan Uesato, Po-Sen Huang, Ramona Comanescu, Fan Yang, Abigail See, Sumanth Dathathri, Rory Greig, Charlie Chen, Doug Fritz, Jaume Sanchez Elias, Richard Green, Soňa Mokrá, Nicholas Fernando, Boxi Wu, Rachel Foley, Susannah Young, Iason Gabriel, William Isaac, John Mellor, Demis Hassabis, Koray Kavukcuoglu, Lisa Anne Hendricks, and Geoffrey Irving. Improving alignment of dialogue agents via targeted human judgements, 2022.
- Caglar Gulcehre, Tom Le Paine, Srivatsan Srinivasan, Ksenia Konyushkova, Lotte Weerts, Abhishek Sharma, Aditya Siddhant, Alex Ahern, Miaosen Wang, Chenjie Gu, et al. Reinforced self-training (rest) for language modeling. *arXiv preprint arXiv:2308.08998*, 2023.
- Tuomas Haarnoja, Aurick Zhou, Pieter Abbeel, and Sergey Levine. Soft actor-critic: Off-policy maximum entropy deep reinforcement learning with a stochastic actor. *CoRR*, abs/1801.01290, 2018. URL <http://arxiv.org/abs/1801.01290>.
- Matthew J. Hausknecht, Prithviraj Ammanabrolu, Marc-Alexandre Côté, and Xingdi Yuan. Interactive fiction games: A colossal adventure. *CoRR*, abs/1909.05398, 2019. URL <http://arxiv.org/abs/1909.05398>.
- Joey Hong, Sergey Levine, and Anca Dragan. Zero-shot goal-directed dialogue via rl on imagined conversations, 2023.
- Youngsoo Jang, Jongmin Lee, and Kee-Eung Kim. GPT-critic: Offline reinforcement learning for end-to-end task-oriented dialogue systems. In *International Conference on Learning Representations*, 2022. URL <https://openreview.net/forum?id=qaxhBG1UUaS>.
- Natasha Jaques, Judy Hanwen Shen, Asma Ghandeharioun, Craig Ferguson, Àgata Lapedriza, Noah Jones, Shixiang Shane Gu, and Rosalind W. Picard. Human-centric dialog training via offline reinforcement learning. *CoRR*, abs/2010.05848, 2020. URL <https://arxiv.org/abs/2010.05848>.
- Albert Q. Jiang, Alexandre Sablayrolles, Arthur Mensch, Chris Bamford, Devendra Singh Chaplot, Diego de las Casas, Florian Bressand, Gianna Lengyel, Guillaume Lample, Lucile Saulnier, Léo Renard Lavaud, Marie-Anne Lachaux, Pierre Stock, Teven Le Scao, Thibaut Lavril, Thomas Wang, Timothée Lacroix, and William El Sayed. Mistral 7b, 2023.
- Tomasz Korbak, Kejian Shi, Angelica Chen, Rasika Bhalerao, Christopher L. Buckley, Jason Phang, Samuel R. Bowman, and Ethan Perez. Pretraining language models with human preferences, 2023.

- Ilya Kostrikov, Ashvin Nair, and Sergey Levine. Offline reinforcement learning with implicit q-learning, 2021.
- Aviral Kumar, Justin Fu, Matthew Soh, George Tucker, and Sergey Levine. Stabilizing off-policy q-learning via bootstrapping error reduction. *Advances in Neural Information Processing Systems*, 32, 2019.
- Aviral Kumar, Aurick Zhou, George Tucker, and Sergey Levine. Conservative q-learning for offline reinforcement learning. *CoRR*, abs/2006.04779, 2020. URL <https://arxiv.org/abs/2006.04779>.
- Sungjin Lee, Qi Zhu, Ryuichi Takanobu, Xiang Li, Yaoqin Zhang, Zheng Zhang, Jinchao Li, Baolin Peng, Xiujun Li, Minlie Huang, and Jianfeng Gao. Convlab: Multi-domain end-to-end dialog system platform. In *Proceedings of the 57th Annual Meeting of the Association for Computational Linguistics*, 2019.
- Yujia Li, David H. Choi, Junyoung Chung, Nate Kushman, Julian Schrittwieser, Rémi Leblond, Tom Eccles, James Keeling, Felix Gimeno, Agustin Dal Lago, Thomas Hubert, Peter Choy, Cyprien de Masson d’Autume, Igor Babuschkin, Xinyun Chen, Po-Sen Huang, Johannes Welbl, Sven Gowal, Alexey Cherepanov, James Molloy, Daniel Jaymin Mankowitz, Esme Sutherland Robson, Pushmeet Kohli, Nando de Freitas, Koray Kavukcuoglu, and Oriol Vinyals. Competition-level code generation with alphacode. *Science*, 378:1092 – 1097, 2022. URL <https://api.semanticscholar.org/CorpusID:246527904>.
- Xi Victoria Lin, Chenglong Wang, Luke Zettlemoyer, and Michael D. Ernst. Nl2bash: A corpus and semantic parser for natural language interface to the linux operating system. *CoRR*, abs/1802.08979, 2018. URL <http://arxiv.org/abs/1802.08979>.
- Xiao Liu, Hao Yu, Hanchen Zhang, Yifan Xu, Xuanyu Lei, Hanyu Lai, Yu Gu, Hangliang Ding, Kaiwen Men, Kejuan Yang, Shudan Zhang, Xiang Deng, Aohan Zeng, Zhengxiao Du, Chenhui Zhang, Sheng Shen, Tianjun Zhang, Yu Su, Huan Sun, Minlie Huang, Yuxiao Dong, and Jie Tang. Agentbench: Evaluating llms as agents, 2023.
- Yinhan Liu, Myle Ott, Naman Goyal, Jingfei Du, Mandar Joshi, Danqi Chen, Omer Levy, Mike Lewis, Luke Zettlemoyer, and Veselin Stoyanov. Roberta: A robustly optimized BERT pretraining approach. *CoRR*, abs/1907.11692, 2019. URL <http://arxiv.org/abs/1907.11692>.
- Volodymyr Mnih, Koray Kavukcuoglu, David Silver, Alex Graves, Ioannis Antonoglou, Daan Wierstra, and Martin A. Riedmiller. Playing atari with deep reinforcement learning. *CoRR*, abs/1312.5602, 2013. URL <http://arxiv.org/abs/1312.5602>.
- Evgenii Nikishin, Max Schwarzer, Pierluca D’Oro, Pierre-Luc Bacon, and Aaron Courville. The primacy bias in deep reinforcement learning. In *International conference on machine learning*, pages 16828–16847. PMLR, 2022.
- OpenAI, :, Josh Achiam, Steven Adler, Sandhini Agarwal, Lama Ahmad, Ilge Akkaya, Florencia Leoni Aleman, Diogo Almeida, Janko Altschmidt, Sam Altman, Shyamal Anadkat, Red Avila, Igor Babuschkin, Suchir Balaji, Valerie Balcom, Paul Baltescu, Haiming Bao, Mo Bavarian, Jeff Belgum, Irwan Bello, Jake Berdine, Gabriel Bernadett-Shapiro, Christopher Berner, Lenny Bogdonoff, Oleg Boiko, Madelaine Boyd, Anna-Luisa Brakman, Greg Brockman, Tim Brooks, Miles Brundage, Kevin Button, Trevor Cai, Rosie Campbell, Andrew Cann, Brittany Carey, Chelsea Carlson, Rory Carmichael, Brooke Chan, Che Chang, Fotis Chantzis, Derek Chen, Sully Chen, Ruby Chen, Jason Chen, Mark Chen, Ben Chess, Chester Cho, Casey Chu, Hyung Won Chung, Dave Cummings,

Jeremiah Currier, Yunxing Dai, Cory Decareaux, Thomas Degry, Noah Deutsch, Damien Deville, Arka Dhar, David Dohan, Steve Dowling, Sheila Dunning, Adrien Ecoffet, Atty Eleti, Tyna Eloundou, David Farhi, Liam Fedus, Niko Felix, Simón Posada Fishman, Juston Forte, Isabella Fulford, Leo Gao, Elie Georges, Christian Gibson, Vik Goel, Tarun Gogineni, Gabriel Goh, Rapha Gontijo-Lopes, Jonathan Gordon, Morgan Grafstein, Scott Gray, Ryan Greene, Joshua Gross, Shixiang Shane Gu, Yufei Guo, Chris Hallacy, Jesse Han, Jeff Harris, Yuchen He, Mike Heaton, Johannes Heidecke, Chris Hesse, Alan Hickey, Wade Hickey, Peter Hoeschele, Brandon Houghton, Kenny Hsu, Shengli Hu, Xin Hu, Joost Huizinga, Shantanu Jain, Shawn Jain, Joanne Jang, Angela Jiang, Roger Jiang, Haozhun Jin, Denny Jin, Shino Jomoto, Billie Jonn, Heewoo Jun, Tomer Kaftan, Łukasz Kaiser, Ali Kamali, Ingmar Kanitscheider, Nitish Shirish Keskar, Tabarak Khan, Logan Kilpatrick, Jong Wook Kim, Christina Kim, Yongjik Kim, Hendrik Kirchner, Jamie Kiros, Matt Knight, Daniel Kokotajlo, Łukasz Kondraciuk, Andrew Kondrich, Aris Konstantinidis, Kyle Kosic, Gretchen Krueger, Vishal Kuo, Michael Lampe, Ikai Lan, Teddy Lee, Jan Leike, Jade Leung, Daniel Levy, Chak Ming Li, Rachel Lim, Molly Lin, Stephanie Lin, Mateusz Litwin, Theresa Lopez, Ryan Lowe, Patricia Lue, Anna Makanju, Kim Malfacini, Sam Manning, Todor Markov, Yaniv Markovski, Bianca Martin, Katie Mayer, Andrew Mayne, Bob McGrew, Scott Mayer McKinney, Christine McLeavey, Paul McMillan, Jake McNeil, David Medina, Aalok Mehta, Jacob Menick, Luke Metz, Andrey Mishchenko, Pamela Mishkin, Vinnie Monaco, Evan Morikawa, Daniel Mossing, Tong Mu, Mira Murati, Oleg Murk, David Mély, Ashvin Nair, Reiichiro Nakano, Rajeev Nayak, Arvind Neelakantan, Richard Ngo, Hyeonwoo Noh, Long Ouyang, Cullen O’Keefe, Jakub Pachocki, Alex Paino, Joe Palermo, Ashley Pantuliano, Giambattista Parascandolo, Joel Parish, Emy Parparita, Alex Passos, Mikhail Pavlov, Andrew Peng, Adam Perelman, Filipe de Avila Belbute Peres, Michael Petrov, Henrique Ponde de Oliveira Pinto, Michael, Pokorny, Michelle Pokrass, Vitchyr Pong, Tolly Powell, Alethea Power, Boris Power, Elizabeth Proehl, Raul Puri, Alec Radford, Jack Rae, Aditya Ramesh, Cameron Raymond, Francis Real, Kendra Rimbach, Carl Ross, Bob Rotsted, Henri Roussez, Nick Ryder, Mario Saltarelli, Ted Sanders, Shibani Santurkar, Girish Sastry, Heather Schmidt, David Schnurr, John Schulman, Daniel Selsam, Kyla Sheppard, Toki Sherbakov, Jessica Shieh, Sarah Shoker, Pranav Shyam, Szymon Sidor, Eric Sigler, Maddie Simens, Jordan Sitkin, Katarina Slama, Ian Sohl, Benjamin Sokolowsky, Yang Song, Natalie Staudacher, Felipe Petroski Such, Natalie Summers, Ilya Sutskever, Jie Tang, Nikolas Tezak, Madeleine Thompson, Phil Tillet, Amin Tootoonchian, Elizabeth Tseng, Preston Tuggle, Nick Turley, Jerry Tworek, Juan Felipe Cerón Uribe, Andrea Vallone, Arun Vijayvergiya, Chelsea Voss, Carroll Wainwright, Justin Jay Wang, Alvin Wang, Ben Wang, Jonathan Ward, Jason Wei, CJ Weinmann, Akila Welihinda, Peter Welinder, Jiayi Weng, Lilian Weng, Matt Wiethoff, Dave Willner, Clemens Winter, Samuel Wolrich, Hannah Wong, Lauren Workman, Sherwin Wu, Jeff Wu, Michael Wu, Kai Xiao, Tao Xu, Sarah Yoo, Kevin Yu, Qiming Yuan, Wojciech Zaremba, Rowan Zellers, Chong Zhang, Marvin Zhang, Shengjia Zhao, Tianhao Zheng, Juntang Zhuang, William Zhuk, and Barret Zoph. Gpt-4 technical report, 2023.

Long Ouyang, Jeff Wu, Xu Jiang, Diogo Almeida, Carroll L. Wainwright, Pamela Mishkin, Chong Zhang, Sandhini Agarwal, Katarina Slama, Alex Ray, John Schulman, Jacob Hilton, Fraser Kelton, Luke E. Miller, Maddie Simens, Amanda Askell, Peter Welinder, Paul Francis Christiano, Jan Leike, and Ryan J. Lowe. Training language models to follow instructions with human feedback. *ArXiv*, abs/2203.02155, 2022. URL <https://api.semanticscholar.org/CorpusID:246426909>.

Romain Paulus, Caiming Xiong, and Richard Socher. A deep reinforced model for abstractive summarization, 2017.

Xue Bin Peng, Aviral Kumar, Grace Zhang, and Sergey Levine. Advantage-weighted regression: Simple and scalable off-policy reinforcement learning. *CoRR*, abs/1910.00177, 2019. URL <http://arxiv.org/abs/1910.00177>.

- Alec Radford, Jeff Wu, Rewon Child, David Luan, Dario Amodei, and Ilya Sutskever. Language models are unsupervised multitask learners. 2019. URL <https://api.semanticscholar.org/CorpusID:160025533>.
- Rafael Rafailov, Archit Sharma, Eric Mitchell, Stefano Ermon, Christopher D. Manning, and Chelsea Finn. Direct preference optimization: Your language model is secretly a reward model, 2023.
- Rajkumar Ramamurthy, Prithviraj Ammanabrolu, Kianté Brantley, Jack Hessel, Rafet Sifa, Christian Bauckhage, Hannaneh Hajishirzi, and Yejin Choi. Is reinforcement learning (not) for natural language processing?: Benchmarks, baselines, and building blocks for natural language policy optimization. 2022. URL <https://arxiv.org/abs/2210.01241>.
- Rajkumar Ramamurthy, Prithviraj Ammanabrolu, Kianté Brantley, Jack Hessel, Rafet Sifa, Christian Bauckhage, Hannaneh Hajishirzi, and Yejin Choi. Is reinforcement learning (not) for natural language processing: Benchmarks, baselines, and building blocks for natural language policy optimization, 2023.
- Marc’Aurelio Ranzato, Sumit Chopra, Michael Auli, and Wojciech Zaremba. Sequence level training with recurrent neural networks, 2015.
- Timo Schick, Jane Dwivedi-Yu, Roberto Dessì, Roberta Raileanu, Maria Lomeli, Luke Zettlemoyer, Nicola Cancedda, and Thomas Scialom. Toolformer: Language models can teach themselves to use tools, 2023.
- John Schulman, Philipp Moritz, Sergey Levine, Michael I. Jordan, and P. Abbeel. High-dimensional continuous control using generalized advantage estimation. *CoRR*, abs/1506.02438, 2015. URL <https://api.semanticscholar.org/CorpusID:3075448>.
- John Schulman, Filip Wolski, Prafulla Dhariwal, Alec Radford, and Oleg Klimov. Proximal policy optimization algorithms. *CoRR*, abs/1707.06347, 2017. URL <http://arxiv.org/abs/1707.06347>.
- Noah Shinn, Federico Cassano, Beck Labash, Ashwin Gopinath, Karthik Narasimhan, and Shunyu Yao. Reflexion: Language agents with verbal reinforcement learning. 2023. URL <https://api.semanticscholar.org/CorpusID:258833055>.
- Charlie Snell, Ilya Kostrikov, Yi Su, Mengjiao Yang, and Sergey Levine. Offline rl for natural language generation with implicit language q learning, 2023.
- Yuda Song, Yifei Zhou, Ayush Sekhari, J. Andrew Bagnell, Akshay Krishnamurthy, and Wen Sun. Hybrid rl: Using both offline and online data can make rl efficient, 2023.
- Richard S Sutton, David McAllester, Satinder Singh, and Yishay Mansour. Policy gradient methods for reinforcement learning with function approximation. In S. Solla, T. Leen, and K. Müller, editors, *Advances in Neural Information Processing Systems*, volume 12. MIT Press, 1999. URL https://proceedings.neurips.cc/paper_files/paper/1999/file/464d828b85b0bed98e80ade0a5c43b0f-Paper.pdf.
- Andrew Szot, Max Schwarzer, Harsh Agrawal, Bogdan Mazouze, Walter Talbott, Katherine Metcalf, Natalie Mackraz, Devon Hjelm, and Alexander Toshev. Large language models as generalizable policies for embodied tasks, 2023.

- Hugo Touvron, Louis Martin, Kevin Stone, Peter Albert, Amjad Almahairi, Yasmine Babaei, Nikolay Bashlykov, Soumya Batra, Prajjwal Bhargava, Shruti Bhosale, Dan Bikel, Lukas Blecher, Cristian Canton Ferrer, Moya Chen, Guillem Cucurull, David Esiobu, Jude Fernandes, Jeremy Fu, Wenyin Fu, Brian Fuller, Cynthia Gao, Vedanuj Goswami, Naman Goyal, Anthony Hartshorn, Saghar Hosseini, Rui Hou, Hakan Inan, Marcin Kardas, Viktor Kerkez, Madian Khabsa, Isabel Kloumann, Artem Korenev, Punit Singh Koura, Marie-Anne Lachaux, Thibaut Lavril, Jenya Lee, Diana Liskovich, Yinghai Lu, Yuning Mao, Xavier Martinet, Todor Mihaylov, Pushkar Mishra, Igor Molybog, Yixin Nie, Andrew Poulton, Jeremy Reizenstein, Rashi Rungta, Kalyan Saladi, Alan Schelten, Ruan Silva, Eric Michael Smith, Ranjan Subramanian, Xiaoqing Ellen Tan, Binh Tang, Ross Taylor, Adina Williams, Jian Xiang Kuan, Puxin Xu, Zheng Yan, Iliyan Zarov, Yuchen Zhang, Angela Fan, Melanie Kambadur, Sharan Narang, Aurelien Rodriguez, Robert Stojnic, Sergey Edunov, and Thomas Scialom. Llama 2: Open foundation and fine-tuned chat models, 2023.
- Hado van Hasselt, Arthur Guez, and David Silver. Deep reinforcement learning with double q-learning. *CoRR*, abs/1509.06461, 2015. URL <http://arxiv.org/abs/1509.06461>.
- Siddharth Verma, Justin Fu, Mengjiao Yang, and Sergey Levine. Chai: A chatbot ai for task-oriented dialogue with offline reinforcement learning, 2022.
- Guanzhi Wang, Yuqi Xie, Yunfan Jiang, Ajay Mandlekar, Chaowei Xiao, Yuke Zhu, Linxi (Jim) Fan, and Anima Anandkumar. Voyager: An open-ended embodied agent with large language models. *ArXiv*, abs/2305.16291, 2023. URL <https://api.semanticscholar.org/CorpusID:258887849>.
- Ronald J. Williams. Simple statistical gradient-following algorithms for connectionist reinforcement learning. *Machine Learning*, 8:229–256, 2004. URL <https://api.semanticscholar.org/CorpusID:19115634>.
- Yuxiang Wu and Baotian Hu. Learning to extract coherent summary via deep reinforcement learning, 2018.
- Tengyang Xie, Ching-An Cheng, Nan Jiang, Paul Mineiro, and Alekh Agarwal. Bellman-consistent pessimism for offline reinforcement learning. *CoRR*, abs/2106.06926, 2021. URL <https://arxiv.org/abs/2106.06926>.
- John Yang, Akshara Prabhakar, Karthik Narasimhan, and Shunyu Yao. Intercode: Standardizing and benchmarking interactive coding with execution feedback, 2023a.
- Kaiyu Yang, Aidan M Swope, Alex Gu, Rahul Chalamala, Peiyang Song, Shixing Yu, Saad Godil, Ryan Prenger, and Anima Anandkumar. LeanDojo: Theorem Proving with Retrieval-Augmented Language Models. *arXiv preprint arXiv:2306.15626*, 2023b.
- Shunyu Yao, Howard Chen, John Yang, and Karthik Narasimhan. Webshop: Towards scalable real-world web interaction with grounded language agents, 2023a.
- Shunyu Yao, Jeffrey Zhao, Dian Yu, Nan Du, Izhak Shafran, Karthik Narasimhan, and Yuan Cao. React: Synergizing reasoning and acting in language models, 2023b.
- Zheng Yuan, Hongyi Yuan, Chuanqi Tan, Wei Wang, Songfang Huang, and Fei Huang. Rrhf: Rank responses to align language models with human feedback without tears, 2023.
- Andrea Zanette. When is realizability sufficient for off-policy reinforcement learning?, 2023.
- Aohan Zeng, Mingdao Liu, Rui Lu, Bowen Wang, Xiao Liu, Yuxiao Dong, and Jie Tang. Agenttuning: Enabling generalized agent abilities for llms, 2023.

Wenhao Zhan, Baihe Huang, Audrey Huang, Nan Jiang, and Jason D. Lee. Offline reinforcement learning with realizability and single-policy concentrability, 2022.

Shuyan Zhou, Frank F. Xu, Hao Zhu, Xuhui Zhou, Robert Lo, Abishek Sridhar, Xianyi Cheng, Yonatan Bisk, Daniel Fried, Uri Alon, and Graham Neubig. Webarena: A realistic web environment for building autonomous agents. *ArXiv*, abs/2307.13854, 2023a. URL <https://api.semanticscholar.org/CorpusID:260164780>.

Yifei Zhou, Ayush Sekhari, Yuda Song, and Wen Sun. Offline data enhanced on-policy policy gradient with provable guarantees, 2023b.

Qi Zhu, Zheng Zhang, Yan Fang, Xiang Li, Ryuichi Takanobu, Jinchao Li, Baolin Peng, Jianfeng Gao, Xiaoyan Zhu, and Minlie Huang. Convlab-2: An open-source toolkit for building, evaluating, and diagnosing dialogue systems. *CoRR*, abs/2002.04793, 2020. URL <https://arxiv.org/abs/2002.04793>.

Daniel M. Ziegler, Nisan Stiennon, Jeffrey Wu, Tom B. Brown, Alec Radford, Dario Amodei, Paul F. Christiano, and Geoffrey Irving. Fine-tuning language models from human preferences. *CoRR*, abs/1909.08593, 2019. URL <http://arxiv.org/abs/1909.08593>.

Appendices

A. Environment and Dataset Details

In this section, we provide more details on the environments and datasets that we used in our experiments. Example actions and observations for each environment are shown in Figure 6.

Detective Game (Hausknecht et al., 2019). In this game, the agent plays the role of a detective looking into a case where the Mayor got murdered. At each time step, the agent generates a free-form text where the game engine parses the text and determines the next state at each time step. The game engine provides a feedback of “Illegal Action.” if the generated text is an illegal action or cannot be correctly parsed. The optimal policy takes 51 steps to solve and reaches a maximum reward of 360. The game timeouts and terminates after 60 steps (including steps where illegal actions are generated). The observation at each time step includes the current surroundings, items carried, environment feedback for the outcome of the last action, and a list of available actions. The Supervised Fine-Tuning (SFT) dataset for this environment consists of 1000 trajectories of an agent picking a random action from the list of available actions at each timestep.

<p style="text-align: center;">Detective Game</p> <p>Action: take paper</p> <p>Observation:</p> <p><< Chief's office >> You are standing in the Chief's office. He is telling you "The Mayor was murdered yeaterday night at 12:03 am. I want you to solve it before we get any bad publicity or the FBI has to come in. "Yessir!" You reply. He hands you a sheet of paper. Once you have read it, go north or west.</p> <p>You are carrying: a piece of white paper</p> <p>Taken.</p> <p>[Your score has just gone up by ten points.] ['east', 'west', 'put paper down', 'north']</p>	<p style="text-align: center;">Guess My City</p> <p>Action: Is your city located in Europe?</p> <p>Observation:</p> <p>Questions: What is the primary language spoken in your city? The primary language spoken in the city is Spanish.</p> <p>Is your city located on the east coast of the country? Yes, it is located on the east coast of the country.</p> <p>Is your city located in North America? No, my city is not located in North America.</p> <p>Is your city located in Europe? Yes, my city is located in Europe.</p>
<p style="text-align: center;">Twenty Questions</p> <p>Action: Is the object an artwork?</p> <p>Observation:</p> <p>Questions: Is the object alive? No. Is the object man-made? Yes. Is the object a vehicle? No. Is the object a piece of furniture? No. Is the object a piece of clothing? No. Is the object a piece of technology? No. Is the object a piece of jewelry? No. Is the object a piece of clothing? No. Is the object an artwork? No.</p>	<p style="text-align: center;">Web Shopping</p> <p>Action:</p> <p>search[wireless bluetooth 4.0 power amplifier board]</p> <p>Observation:</p> <p>WebShop Instruction: i am looking for a wireless bluetooth 4.0 power amplifier board, and price lower than 60.00 dollars [Search] Action: search[wireless bluetooth 4.0 power amplifier board] Observation: [Back to Search] Page 1 (Total results: 50) [Next >] [B08LDPQCB4] Audio Amplifier Module,TDA7492P Wireless Bluetooth 4.0 Audio Receiver Power Amplifier Board Module,CSR8635 Bluetooth Chip,Auto Pairing,Amplifier Speakers Board \$25.19 [B08GPVK8LB] Liccx TDA7492P Power Amplifier Board£-Wireless Bluetooth 4.0 Audio Receiver Power Amplifier Board Module Audio Amplifier Module \$24.99</p>

Figure 6: Example actions and observations for each environment that we study in this paper.

Twenty Questions and Twenty Questions Subset (Abdulhai et al., 2023). In this environment, for each episode, a random word is chosen from a list of 157 words of household items such as “basketball”, “apple”, and “car”. The word is held hidden from the agent and the agent is tasked to guess the hidden word within 20 questions. The questions are limited to yes/no questions and the answers from the oracle are limited to “Yes.”, “No.”, and “Invalid Question.”. As opposed to using “flan-t5-xl”(Chung et al., 2022) as the oracle (Abdulhai et al., 2023), we train a ‘flan-t5-small’ to simulate the oracle with the same data and use it for our online experiments due to computational constraints. The agent gets a reward of 0 if it guesses the correct word and the episode terminates. Otherwise, the agent gets a reward of -1 for each question it raises. This reward structure results in a minimum reward of -20 if the agent does not guess the correct word with twenty questions and a maximum reward of 0 if the agent guesses the correct word with the first question although it is very unlikely. We use the official offline dataset provided by Abdulhai et al. (2023) with 100K simulated episodes. Our SFT checkpoints for online experiments for both Twenty Questions and Twenty Questions Subset are also trained with this dataset. Twenty Questions Subset keeps everything else the same except that it uses a subset of 10 hidden words in the word list. Since the offline dataset and the SFT checkpoint for online experiments are based on the entire Twenty Questions, Twenty Questions Subset challenges different algorithms with a significant distribution shift and requires the agent to come up with an entirely different strategy from behavior cloning.

Guess My City (Abdulhai et al., 2023). This environment is a similar dialogue task to Twenty Questions. For each episode, a random city is chosen from a list of 100 cities in the world. The city is held hidden from the agent and the agent is tasked to guess the name of the city within 20 questions. Both the questions and answers are free-form except that the answers are not allowed to contain the name of the city. As opposed to using “flan-t5-xl”(Chung et al., 2022) as the oracle (Abdulhai et al., 2023), we train a ‘flan-t5-small’ to simulate the oracle with the same data and use it for our online experiments due to computational constraints. We found in our online experiments that the agent can easily learn to “exploit” the oracle by tricking it to directly output the name of the city. Therefore, we simply replace the answer with a hardcoded template “I cannot answer that question.” if the name of the city is found in the output of the oracle language model to reduce reward hacking. The reward structure is the same as Twenty Questions. We use the official offline dataset provided by Abdulhai et al. (2023) with 100K simulated episodes.

Web Shopping (Yao et al., 2023a). This environment challenges the ability of the agents to interact with external tools. For each episode, a random instruction requesting a specific item is chosen and shown to the agent. The agent needs to make use of a simplified web shopping server to make the purchase. Every successful purchase is consisted of searching the keywords in the search engine, selecting an item from searched results, clicking on features and attributes for the item, and finally making the purchase. Following ReAct (Yao et al., 2023b), the agent can choose to take a “think” action before taking any actual actions such as “search” and “click”. An observation consists of the instruction and the history of visited webpages (described in text) and actions. The reward is a scalar between 0 and 1 depending on the similarity of the purchased item with the requested item. For example, a partial reward will be given if the agent purchases a black king-sized bed while a black queen-sized bed is requested. The episode timeouts after 10 interaction steps and a reward of 0 is issued. Our main online environments use a subset of 100 instructions from index 2000 to 2100 for a fast evaluation. We collect the offline dataset using the instructions from index 0 to 1000 with GPT-3 text-davinci-002 with prompts from ReAct’s official implementation.

B. Offline Algorithm and Practical Considerations

Our offline algorithm is a hierarchical version of the IQL algorithm (Kostrikov et al., 2021). Specifically, the critic leverages IQL (Eq. (6)) while the actor update is based on AWR (Equation 7).

These choices for the actor and for the critic update identify two key hyperparameters, the expectile value τ (defined in Equation 6 and 7) and the temperature β , whose effect is described in the respective sections. These hyper-parameters are already present in the original IQL algorithm (Kostrikov et al., 2021), and they have a similar interpretation here. By choosing τ and β appropriately, the algorithm identifies a policy whose performance should be between the optimal one and the one that generated the dataset. (In general, recovering the optimal policy by just using a dataset may not be possible as the dataset may not contain information about an optimal policy).

The offline algorithm shares most of the ingredients with its online counterpart, such as the double critic, target networks, soft updates, and value function heads. However, some unique features inherited from IQL allow to considerably simplify several algorithmic choices.

- The actor and the critic no longer need to be synchronized by using a certain update ratio. This is because the critic update defined in Equation 6 is independent of the actor’s current policy, and so the two can be updated with any desired frequency without introducing instabilities.
- It is not necessary to pre-train the policy with a behavioural cloning objective, because such objective is already included in the actor’s loss function in Equation 7.
- The warmup steps for the critic are also not necessary, because the initially small advantage function has a negligible effect in the AWR loss.

C. Additional Baseline Details

C.1. Performance of PPO

In Figure 7, we provide a zoom-in of the learning curves of PPO for Twenty Questions, Twenty Questions Subset, and Guess My City. We observed that PPO does improve over the SFT checkpoint, especially in the more simple task Twenty Questions Subset. However, as PPO is unable to reuse past off-policy data, we need to collect at least 1024 trajectories of on-policy data for each PPO update, as shown in Appendix F. This observation is consistent with Abdulhai et al. (2023).

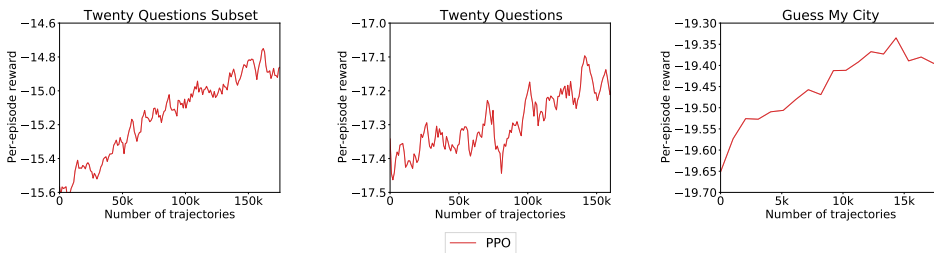


Figure 7: A zoom-in of learning curves of PPO. PPO gradually improves despite its worse sample complexity compared to other off-policy methods.

C.2. Additional Reproduction Details for WebShop Experiment

For our WebShop experiment, we utilized the environment and the few-shot prompting baselines from ReAct (Yao et al., 2023b). ReAct introduces two prompting strategies: the ReAct method and the Act-only method, which we denote as *ReAct* and *expert-prompt* in Figure 4. The ReAct method

additionally allows the agent to articulate its reasoning before making an action, whereas the Act-only method does not. We use the original prompts in ReAct’s implementation without any modifications, and to ensure that our paper is self-contained, we also include these prompts in Figure 9 and 8.

We assessed these algorithms on the webshop index from 2000 to 2100 to establish the LLM-based few-shot baselines in Figure 4. Notably, by early January 2024, OpenAI had deprecated the GPT-3 text-davinci-002 model used in the original ReAct study. Consequently, we switched to the gpt-3.5-turbo-instruct model. While the expert-prompt approach yielded performance comparable to the best performing text-davinci-002 based method, the ReAct method underperformed significantly with the newer model. This discrepancy, also observed and replicated in other tasks independently by other researchers¹, is faithfully depicted in Figure 4.

¹For more details, see the Github Issue on ReAct’s repository: <https://github.com/ysmyth/ReAct>

ReAct Prompt

Webshop

Instruction:

i would like a 3 ounce bottle of bright citrus deodorant for sensitive skin, and price lower than 50.00 dollars

[Search]

Action: search[3 ounce bright citrus deodorant sensitive skin]

Observation:

[Back to Search]

Page 1 (Total results: 50)

[Next >]

[B078GWRC1J]

Bright Citrus Deodorant by Earth Mama | Natural and Safe for Sensitive Skin, Pregnancy and Breastfeeding, Contains Organic Calendula 3-Ounce

\$10.99

[B078GTKVXY]

Ginger Fresh Deodorant by Earth Mama | Natural and Safe for Sensitive Skin, Pregnancy and Breastfeeding, Contains Organic Calendula 3-Ounce

\$10.99

[B08KBVJ4XN]

Barrel and Oak - Aluminum-Free Deodorant, Deodorant for Men, Essential Oil-Based Scent, 24-Hour Odor Protection, Cedar & Patchouli Blend, Gentle on Sensitive Skin (Mountain Sage, 2.7 oz, 2-Pack)

\$15.95

Action: think[B078GWRC1J and B078GTKVXY are bright citrus deodorant less then 50 dollars. I can check B078GWRC1J first.]

Observation: OK.

Action: click[B078GWRC1J]

Observation:

[Back to Search]

[< Prev]

scent [assorted scents][bright citrus][calming lavender][ginger fresh][simply non-scents]
size [travel set (4-pack)][3 ounce (pack of 1)][3-ounce (2-pack)]

Bright Citrus Deodorant by Earth Mama | Natural and Safe for Sensitive Skin, Pregnancy and Breastfeeding, Contains Organic Calendula 3-Ounce

Price: \$10.99

Rating: N.A.

[Description]

[Features]

[Reviews]

[Buy Now]

Action: think[For 3 ounce bottle of bright citrus deodorant for sensitive skin, the item has options 'bright citrus' and '3 ounce (pack of 1)' and seems good to buy.]

Observation: OK.

Action: click[bright citrus]

Observation: You have clicked bright citrus.

Action: click[3 ounce (pack of 1)]

Observation: You have clicked 3 ounce (pack of 1).

Action: click[Buy Now]

Figure 8: Prompts used by the act-only (expert) baseline.

Act-only (expert) Prompt

Instruction:

i would like a 3 ounce bottle of bright citrus deodorant for sensitive skin, and price lower than 50.00 dollars

[Search]

Action: search[3 ounce bright citrus deodorant sensitive skin]

Observation:

[Back to Search]

Page 1 (Total results: 50)

[Next >]

[B078GWRC1J]

Bright Citrus Deodorant by Earth Mama | Natural and Safe for Sensitive Skin, Pregnancy and Breastfeeding, Contains Organic Calendula 3-Ounce

\$10.99

[B078GTKVXY]

Ginger Fresh Deodorant by Earth Mama | Natural and Safe for Sensitive Skin, Pregnancy and Breastfeeding, Contains Organic Calendula 3-Ounce

\$10.99

[B08KBVJ4XN]

Barrel and Oak - Aluminum-Free Deodorant, Deodorant for Men, Essential Oil-Based Scent, 24-Hour Odor Protection, Cedar & Patchouli Blend, Gentle on Sensitive Skin (Mountain Sage, 2.7 oz, 2-Pack)

\$15.95

Action: click[B078GWRC1J]

Observation:

[Back to Search]

[< Prev]

scent [assorted scents][bright citrus][calming lavender][ginger fresh][simply non-scents]

size [travel set (4-pack)][3 ounce (pack of 1)][3-ounce (2-pack)]

Bright Citrus Deodorant by Earth Mama | Natural and Safe for Sensitive Skin, Pregnancy and Breastfeeding, Contains Organic Calendula 3-Ounce

Price: \$10.99

Rating: N.A.

[Description]

[Features]

[Reviews]

[Buy Now]

Action: click[bright citrus]

Observation: You have clicked bright citrus.

Action: click[3 ounce (pack of 1)]

Observation: You have clicked 3 ounce (pack of 1).

Action: click[Buy Now]

Figure 9: Prompts used by the act-only (expert) baseline.

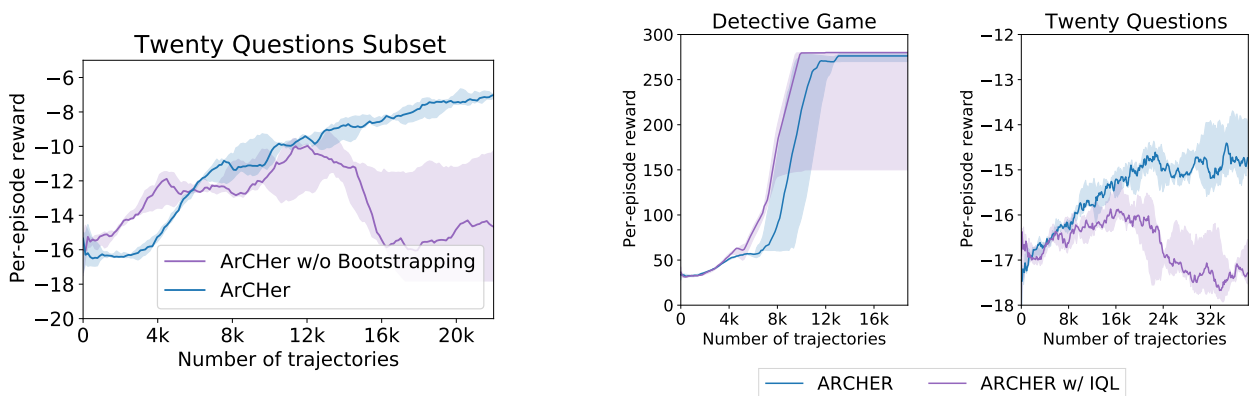
D. Additional Experimental Results

D.1. TD-Learning v.s. MC Regression

To validate whether TD-learning plays an important role in ArCHer, we carried out an ablation study where we replaced TD-learning in ArCHer with MC regression for critic updates. To make sure that data in the replay buffer are generated by similar policies, we use a smaller replay buffer that contains trajectories collected by three latest policies. The ablation results are shown in Figure 10a. We observed that MC regression may learn faster in the beginning as the information propagates faster than per step TD learning, but it fails to learn reliably over the entire training process. This ablation result shows the importance of TD-learning to effectively make use of off-policy data.

D.2. Online IQL Critic Loss

In our ablation study of using IQL critic loss in the online setting, we set $\tau = 0.9$ to encourage more risk-seeking for better explorations. As we can see from Figure 10b, the use of IQL critic can indeed accelerate explorations in simple tasks such as Detective Game. However, a naive instantiation of IQL fails to provide an unbiased estimate for the policy gradient resulting in potential instabilities in harder tasks such as Twenty Questions.



(a) Ablation study of replacing ArCHer critic update with MC Regression. As data in the replay buffer is generated by different policies, MC regression fails to improve reliably.

(b) Ablation study of replacing ArCHer critic update with an IQL loss. Using an IQL critic loss can sometimes accelerate training but introduce more instability.

E. Reward Hacking

To understand whether our agent has really learnt to behave more strategically with reinforcement learning instead of exploiting the environment, we present sample trajectories for Twenty Questions Subset, Twenty Questions, Guess My City, and WebShop in Figure 11, 12, 13, 14. Note that for detective game, there is only a limited number of legal actions and all illegal actions will lead to making no progress in the game, resulting in a lower rewards. For Twenty Questions Subset and Twenty Questions, we observed that the successful dialogues tend to be mostly natural and strategic while some unsuccessful dialogues tend to contain more meaningless repetitions. For Guess My City, we observed that the agent learnt to ask the predominant language of the city which is one of the most informative questions in the SFT distribution we considered in Appendix A. However, as there are some vulnerabilities and hallucinations of the imperfect oracle model for generating free-form answers, some of the conversations might diverge to meaningless repetitions in the end. For WebShop, as the environment forces the format of legal actions for the web server to process, the trajectories

tend to be natural and realistic.

Twenty Questions Subset

Questions:

Is it a living thing? No.

Is it a man-made? Yes.

Is it a machine? No.

Is it a tool? No.

Is it a piece of clothing? No.

Is it a piece of furniture? Yes.

Is it a chair? Yes.

Figure 11: Example environment interactions of ArCHer for Twenty Questions Subset at the end of training. It can be seen that in this environment, ArCHer learnt a near-optimal binary search strategy.

Twenty Questions

Questions:

Is it a living thing? Yes.
 Is the object a mammal? No.
 Is the object a plant? Yes.
 Is the object edible? Yes.
 Is the object a vegetable? No.
 Is the object a fruit? Yes.
 Is the object a citrus fruit? No.
 Is the object a berry? Yes.
 Is the object a strawberry? No.
 Is the object a strawberry? No.
 Is the object a blueberry? No.
 Is the object a rasepeberry? No.
 Is the object a currant? No.
 Is the object a grape? Yes.

Questions:

Is the object a living thing? No.
 Is the object man-made? Yes.
 Is the object a vehicle? No.
 Is the object a piece of jewelry? No.
 Is the object a musical instrument? Yes.
 Is the object a stringed instrument? No.
 Is the object a wind instrument? Yes.
 Is the object a trumpet? No.
 Is the object a trombone? No.
 Is the object a flute? No.
 Is the object a saxophone? No.
 Is the object a clarinet? No.
 Is the object a clarinet? No.
 Is the object a clarinet? No.
 Is the object a clarinet? No.
 Is the object a clarinet? No.
 Is the object a clarinet? No.
 Is the object a clarinet? No.
 Is the object a clarinet? No.

Figure 12: Example environment interactions of ArCHer for Twenty Questions (one successful and one unsuccessful trajectory) at the end of training. In this environment, the conversation is smooth and natural for successful trajectories. However, for unsuccessful trajectories, the agent may sometimes keep repeating the same question.

Guess My City

Questions:

What is the predominant language spoken:

The predominant language spoken is Mandarin Chinese.

Is the city you are from Shanghai?

No, I am not from Shanghai.

Is the city you are from Taipei,Is the city you are from TaipeiIs the city you are from TaipeiIs the city you are from Taipei

Yes

Questions:

What is the predominant language spoken:

English

Is the city you are from London?

No, I am not from London.

Is the city you are from LondonIs the city you are from London Is the city you are from London

Yes, my city is from London.

Is the city you are from LondonIs the city you are from London Is the city you are from London

Yes, my city is from London.

Is the city you are from LondonIs the city you are from London Is the city you are from London

Yes, my city is from London.

Is the city you are from LondonIs the city you are from London Is the city you are from London

Yes, my city is from London.

Is the city you are from LondonIs the city you are from London Is the city you are from London

Yes, my city is from London.

.....

Figure 13: Example environment interactions of ArCHer for Guess My City at the end of training. The agent learns to ask the question for the predominant language, which is one of the most informative questions from the offline SFT distribution. However, as the oracle model provides free-form responses can be out of distribution, the agent is more prone to collapsing in out-of-distribution states.

WebShop

Observation:

WebShop

Instruction:

i would like a citrus yao conditioner made with natural ingredients, and price lower than 50.00 dollars

[Search]

Action:

search[citrus yao conditioner natural ingredients]

Observation:

[Back to Search]

Page 1 (Total results: 50)

[Next >]

[B099KWBV49]

VIORI Terrace Garden Conditioner Bar - Handcrafted with Longsheng Rice Water & Natural Ingredients - Sulfate-free, Paraben-free, Cruelty-free, Phthalate-free, pH balanced 100% Vegan, Zero-Waste

\$16.25

[B09KQZ9GTK]

VIORI Hidden Waterfall Shampoo & Conditioner Bar Set WITHOUT Bamboo Holder - Handcrafted with Longsheng Rice Water & Natural Ingredients - Sulfate-free, Paraben-free, Phthalate-free, 100% Vegan

\$29.25

Action:

click[B099KWBV49]

Observation:

[Back to Search]

[< Prev]

style [bamboo bar holder][citrus yao][hidden waterfall]

size [bamboo bar holder][conditioner][shampoo][shampoo + conditioner set]

VIORI Terrace Garden Conditioner Bar - Handcrafted with Longsheng Rice Water & Natural Ingredients - Sulfate-free, Paraben-free, Cruelty-free, Phthalate-free, pH balanced 100% Vegan, Zero-Waste

Price: \$16.25

Rating: N.A.

[Description]

[Features]

[Reviews]

[Attributes]

[Buy Now]

Action:

click[citrus yao]

Observation:

You have clicked citrus yao.

Action:

click[Buy Now]

Observation:

Your score (min 0.0, max 1.0): 0.75

Figure 14: Example environment interactions of ArCHer for WebShop at the end of training. It can be seen that in this environment, the behavior of ArCHer is very natural.

F. Hyperparameters

Table 2 shows hyperparameters for ArCHer and other baselines for all environments. As shown in the table, most hyperparameters are held the same across all environment except that a smaller actor learning rate is used for Twenty Questions and a larger number of rollout trajectories is used for Web Shopping. This shows that ArCHer is relatively insensitive to selection of hyperparameters and does not require too much hyperparameter tuning to work in different environments.

Table 2: Hyperparameters for All Experiments

		Detective Game	Twenty Questions Subset	Twenty Questions	Guess My City	Web Shopping
SFT	actor lr	2e-4	2e-4	2e-4	2e-4	2e-4
	batch size	32	32	32	32	32
Filtered BC	actor lr	3e-4	3e-4	3e-5	3e-4	3e-4
	batch size	256	256	256	256	256
	rollout trajectories	32	32	32	32	128
	replay buffer size	10000	10000	10000	10000	10000
	filtering percentage	0.1	0.1	0.1	0.1	0.1
	actor updates per iteration	10	10	10	10	10
CHAI	actor lr	3e-4	3e-4	3e-5	3e-4	3e-4
	critic lr	6e-4	6e-4	6e-4	6e-4	6e-4
	batch size	256	256	256	256	256
	rollout trajectories	128	128	128	128	512
	replay buffer size	10000	10000	10000	10000	10000
	critic updates per iteration	50	50	50	50	50
	discount	0.98	0.95	0.95	0.95	0.9
	polyak alpha	0.9	0.9	0.9	0.9	0.9
ArCHer	actor lr	3e-4	3e-4	3e-5	3e-4	3e-4
	critic lr	6e-4	6e-4	6e-4	6e-4	6e-4
	batch size	256	256	256	256	256
	rollout trajectories	128	128	128	128	512
	replay buffer size	10000	10000	10000	10000	10000
	critic updates per iteration	50	50	50	50	50
	discount	0.98	0.95	0.95	0.95	0.9
	polyak alpha	0.9	0.9	0.9	0.9	0.9
	actor updates per iteration	3	3	3	3	3
	warm up iters with no actor update	10	10	20	10	20
	ArCHer w/ Baseline	actor lr	\	\	\	3e-4
critic lr		\	\	\	6e-4	\
batch size		\	\	\	256	\
rollout trajectories		\	\	\	128	\
replay buffer size		\	\	\	10000	\
critic updates per iteration		\	\	\	50	\
discount		\	\	\	0.95	\
actor updates per iteration		\	\	\	3	\
baseline updates per iteration		\	\	\	60	\
warm up iters with no actor update		\	\	\	10	\
polyak alpha		\	\	\	0.9	\
PPO	actor lr	\	6e-6	6e-6	6e-4	\
	batch size	\	1024	1024	1024	\
	rollout trajectories	\	2048	2048	1024	\
	PPO epochs	\	10	20	4	\
	discount	\	0.95	0.95	0.95	\
	GAE lambda	\	0.95	0.95	0.95	\
	clip range	\	0.2	0.2	0.2	\

Table 3: Hyperparameters for ArCHer and baseline methods for all experiments.

G. Proof of Main Theorem

G.1. Equivalent Utterance and Token Level MDPs

We consider the groundtruth utterance-level discounted infinite horizon MDP $\mathcal{M} = \{\mathcal{S}, \mathcal{A}, \gamma, r, \mu_0, P\}$ as defined in Section 3.1. An equivalent token-level infinite horizon MDP can be constructed with

$\tilde{\mathcal{M}} = \{\tilde{\mathcal{S}}, \tilde{\mathcal{A}}, \gamma^{1/L}, r, \mu_0, \tilde{P}\}$, where L is the length of each utterance, $\tilde{\mathcal{A}}$ contains all individual tokens with a special padding token (such that each utterance is padded to the same length L), $\tilde{\mathcal{S}} \in \mathcal{S} \times \tilde{\mathcal{A}}^L$ contains both the state in the utterance-level MDP and the partial sequence of utterance that has already been generated, $\gamma^{1/L}$ is the equivalent discount factor. Note that this definition of token-level MDP is not the same as the definition of token-level MDP in the hierarchical language MDP defined for ArCHer in Section 3.1. The token-level MDP for ArCHer is only embedded in one particular utterance and the only reward that it receives is at the end of the utterance from the utterance-level critic while the equivalent token-level MDP spans multiple utterances and receives rewards from the external environment at the end of each utterance. This construction of token-level MDP is “equivalent” to the utterance-level MDP in the sense that for any autoregressive policy π that generates an utterance token by token, we have:

$$\forall s \in \mathcal{S}, V^\pi(s) = \tilde{V}^\pi(s),$$

where V^π and \tilde{V}^π are value functions of π in the utterance-level MDP \mathcal{M} and the token-level MDP $\tilde{\mathcal{M}}$ respectively. We use $\tilde{\pi}$ for the same utterance-level policy π when it generates one token at a time.

As usual, for any MDP \mathcal{M} , we define $d^\pi \in \Delta(\mathcal{S} \times \mathcal{A})$ as the average state-action occupancy measure of policy π such that:

$$d^\pi(s, a) = (1 - \gamma)(\mu_0(s)\pi(a|s) + \sum_{t=1}^{\infty} \gamma^t P^\pi(s_t = s, a_t = a))$$

We denote $V^\pi = \mathbb{E}_{s_0 \sim \mu_0} V^\pi(s_0)$ as the expected total discounted reward of π . We denote \mathcal{T}^π as the Bellman operator associated with π , i.e., given a function $f \in \mathcal{S} \times \mathcal{A} \mapsto \mathbb{R}$, we have

$$\mathcal{T}^\pi f(s, a) = r(s, a) + \gamma \mathbb{E}_{s' \sim P(s, a), a' \sim \pi(s')} [f(s', a')].$$

Similar definitions can be made in the token-level MDP $\tilde{\mathcal{M}}$ for \tilde{d}^π , \tilde{V}^π , and $\tilde{\mathcal{T}}^\pi$. We also define \tilde{A}^π as the advantage function in the token level.

G.2. Fitted Policy Evaluation Subroutine

In this section, we present our theoretical subroutine for fitting the critic in Algorithm 2. On a high level, it just repeats finding the Q function that minimizes the bellman error with respect to the Q function in the last iteration, and returns the average of all Q functions in the end. Both critic fitting in the token-level MDP $\tilde{\mathcal{M}}$ or in the utterance-level MDP \mathcal{M} follows from the same subroutine with the same function class \mathcal{F} that map the space of sequences of tokens to real values. This theoretical algorithm is simply a more formalized version of the critic update in Algorithm 1.

G.3. Assumptions

We present the two important assumptions that we use for analyzing FPE subroutine, and both assumptions share the same definition for utterance-level MDP \mathcal{M} and token-level MDP $\tilde{\mathcal{M}}$.

Assumption 1 (Bellman Completeness (Song et al., 2023; Zhou et al., 2023b; Zanette, 2023; Xie et al., 2021)). *We say that \mathcal{F} is Bellman Complete for some policy π , if for all $f \in \mathcal{F}$, there exists a $f' \in \mathcal{F}$ such that $\|f'(s, a) - \mathcal{T}^\pi f(s, a)\|_\infty = 0$.*

Assumption 2 (Density Ratio Coefficient (Zhan et al., 2022; Foster et al., 2021)). *Given the offline distribution ν , for any policy π , we define the density ratio coefficient as*

$$C_{\nu, \pi} := \max_{s, a} \frac{d^\pi(s, a)}{\nu(s, a)}.$$

Algorithm 2 Fitted Policy Evaluation (FPE)**Require:** Policy π , function class \mathcal{F} , number of iterations K , weight λ **Require:** K independent datasets $\mathcal{D}_{1:K} = \{(s, a, r, s')\}$ of M many samples each from the same offline distribution ν .

- 1: Initialize $f_0 \in \mathcal{F}$.
- 2: **for** $k = 1, \dots, K$ **do**
- 3: Solve the square loss regression problem to compute:

$$f_k \leftarrow \operatorname{argmin}_{f \in \mathcal{F}} \widehat{\mathbb{E}}_{\mathcal{D}_k} [(f(s, a) - r - \gamma f_{k-1}(s', \pi(s')))]^2 \quad (8)$$

4: **end for**5: **Return** $\bar{f} = \frac{1}{K} \sum_{k=1}^K f_k$.

The following two lemmas compare the utterance-level assumptions and token-level assumptions.

Lemma 1. *For any stationary policy π , token-level Bellman Completeness for $\widetilde{\mathcal{M}} \implies$ utterance-level Bellman Completeness for \mathcal{M}*

Proof. $\forall s \in \mathcal{S}, a \in \mathcal{A}$ being state and action in the utterance-level, the utterance a can be decomposed into L tokens in the action space of the token-level MDP:

$$a = \widetilde{a}_{1:L}, \widetilde{a}_i \in \widetilde{\mathcal{A}}, i = 1, \dots, L.$$

Therefore,

$$\begin{aligned} & \min_{f' \in \mathcal{F}} |f'(s, a) - \mathcal{T}^\pi f'(s, a)| \\ = & \min_{f_1, \dots, f_L \in \mathcal{F}} |f_1(s, a) - \widetilde{\mathcal{T}}^\pi f_2(s, a) + r(s, a) + \gamma^{1/L} \mathbb{E}_{s' \sim P(\cdot|s, a), \widetilde{a}_1 \sim \widetilde{\pi}(\cdot|s')} f_2(s', \widetilde{a}_1) \\ & - \gamma^{1/L} \mathbb{E}_{s' \sim P(\cdot|s, a), \widetilde{a}_1 \sim \widetilde{\pi}(\cdot|s')} \widetilde{\mathcal{T}}^\pi f_3(s', \widetilde{a}_1) + \dots + \gamma^{(L-1)/L} \mathbb{E}_{s' \sim P(\cdot|s, a), \widetilde{a}_{1:L-1} \sim \widetilde{\pi}(\cdot|s')} f_L(s', \widetilde{a}_{1:L-1}) \\ & - r(s, a) - \gamma^{(L-1)/L} \mathbb{E}_{s' \sim P(\cdot|s, a), \widetilde{a}_{1:L-1} \sim \widetilde{\pi}(\cdot|s')} \widetilde{\mathcal{T}}^\pi f(s', \widetilde{a}_{1:L-1})| \\ \leq & \min_{f_1, \dots, f_L \in \mathcal{F}} |f_1(s, a) - \widetilde{\mathcal{T}}^\pi f_2(s, a)| \sum_{i=2}^L \gamma^{(i-1)/L} \mathbb{E}_{s' \sim P(\cdot|s, a), \widetilde{a}_{1:i-1} \sim \widetilde{\pi}(\cdot|s')} |f^i(s, \widetilde{a}_{1:i-1}) - \widetilde{\mathcal{T}}^\pi((s, \widetilde{a}_{1:i-1})| \\ \leq & 0, \end{aligned}$$

where the last inequality follows from the assumption of token-level Bellman Complete. \square

The next lemma assumes that the offline distribution ν is the same for both token-level MDP and utterance-level MDP, i.e. the token-level transitions are derived by splitting utterance-level transitions. We use $\widetilde{\nu}$ to denote the token-level offline distribution created in this way.

Lemma 2. *For any stationary policy π , and any offline distribution ν , we have Density Ratio Coefficient for token-level $\widetilde{\mathcal{M}} =$ Density Ratio Coefficient for utterance-level \mathcal{M} .*

$$C_{\nu, \pi} = C_{\widetilde{\nu}, \pi}$$

Proof. The proof is constructed by noticing the fact that each token-level state consists of not only the

utterance-level state but also all the tokens that have been generated in the current utterance:

$$\begin{aligned}
 & \max_{\tilde{s} \in \tilde{\mathcal{S}}, \tilde{a} \in \tilde{\mathcal{A}}} \frac{\tilde{d}^\pi(\tilde{s}, \tilde{a})}{\tilde{\nu}(\tilde{s}, \tilde{a})} \\
 &= \max_{s \in \mathcal{S}, \tilde{a}_{1:i-1} \in \tilde{\mathcal{A}}, i \in [1, L]} \frac{\tilde{d}^\pi(s, \tilde{a}_{1:i-1}, \tilde{a}_i)}{\tilde{\nu}(s, \tilde{a}_{1:i-1}, \tilde{a}_i)} \\
 &= \max_{s \in \mathcal{S}, \tilde{a}_{1:L} \in \tilde{\mathcal{A}}} \frac{\tilde{d}^\pi(s, \tilde{a}_{1:L})}{\tilde{\nu}(s, \tilde{a}_{1:L})} \\
 &= \max_{s \in \mathcal{S}, a \in \mathcal{A}} \frac{d^\pi(s, a)}{\nu(s, a)},
 \end{aligned}$$

where the first equation follows by regrouping states and actions as each state in the token-level state space $\tilde{s} \in \tilde{\mathcal{S}} = \mathcal{S} \times \tilde{\mathcal{A}}^L$, and the second equation holds because $\max_b \frac{p(a,b)}{q(a,b)} \geq \frac{p(a)}{q(a)}$. \square

G.4. Proof of Main Theorem

Now we are ready to analyze the sample complexity of Fitted Policy Evaluation in Algorithm 2, the proof of our main theorem makes use of several technical lemmas from Section G.5.

Lemma 3 (Guarantees of FPE). *For the algorithm described in Algorithm 2 with K independent datasets $\mathcal{D}_{1:K} = \{(s, a, r, s')\}$ such that the effective number of samples $N = MK$, if the function class satisfies $\max_{f \in \mathcal{F}, s \in \mathcal{S}, a \in \mathcal{A}} |f(s, a)| < R$, then with probability at least $1 - \delta$ the output value function satisfies:*

$$\mathbb{E}_{s, a \sim d^\pi} [(\bar{f}(s, a) - \mathcal{T}^\pi \bar{f}(s, a))^2] \leq C_{\nu, \pi} \left(\frac{4(R+1)^2}{K} + \frac{256R^2 \log(2|\mathcal{F}|K/\delta)}{M} \right).$$

Proof. By applying Lemma 6, to each iteration $1, \dots, K$, and apply a union bound over all iterations, we have that:

$$\begin{aligned}
 \forall k, M \mathbb{E}_{s, a \sim \nu} [(f_k(s, a) - \mathcal{T}^\pi f_{k-1}(s, a))^2] &\leq 3M \inf_{f \in \mathcal{F}} \mathbb{E}_{s, a \sim \nu} [(f(s, a) - \mathcal{T}^\pi f_{k-1}(s, a))^2] + 256R^2 \log(2|\mathcal{F}|K/\delta) \\
 \forall k, \mathbb{E}_{s, a \sim \nu} [(f_k(s, a) - \mathcal{T}^\pi f_{k-1}(s, a))^2] &\leq \frac{256R^2 \log(2|\mathcal{F}|K/\delta)}{M}, \tag{9}
 \end{aligned}$$

where the second line holds by Assumption 1. To combine the guarantees that we have from each round to the guarantee of the returned value function \bar{f} :

$$\begin{aligned}
 & \mathbb{E}_{s, a \sim \nu} [(\bar{f}(s, a) - \mathcal{T}^\pi \bar{f}(s, a))^2] \\
 &= \mathbb{E}_{s, a \sim \nu} \left[\left(\frac{1}{K} (f_1(s, a) - \mathcal{T}^\pi f_K(s, a) + \sum_{k=2}^K f_k(s, a) - \mathcal{T}^\pi f_{k-1}(s, a)) \right)^2 \right] \\
 &\leq \frac{1}{K} \mathbb{E}_{s, a \sim \nu} \left[(f_1(s, a) - \mathcal{T}^\pi f_K(s, a))^2 + \sum_{k=2}^K (f_k(s, a) - \mathcal{T}^\pi f_{k-1}(s, a))^2 \right] \\
 &\leq \frac{1}{K} \left[4(R+1)^2 + (K-1) \frac{256R^2 \log(2|\mathcal{F}|K/\delta)}{M} \right] \\
 &\leq \frac{4(R+1)^2}{K} + \frac{256R^2 \log(2|\mathcal{F}|K/\delta)}{M}, \tag{10}
 \end{aligned}$$

where the first inequality follows by Jensen's Inequality and the second inequality follows by plugging in Line 9. Then, we can plug in Assumption 2 to conclude the proof.

$$\begin{aligned}
\mathbb{E}_{s,a \sim d^\pi} [(\bar{f}(s,a) - \mathcal{T}^\pi \bar{f}(s,a))^2] &\leq C_{\nu,\pi} \mathbb{E}_{s,a \sim \nu} [(\bar{f}(s,a) - \mathcal{T}^\pi \bar{f}(s,a))^2] \\
&\leq C_{\nu,\pi} \left(\frac{4(R+1)^2}{K} + \frac{256R^2 \log(2|\mathcal{F}|K/\delta)}{M} \right). \\
&\leq 64C_{\nu,\pi} R(R+1) \sqrt{\frac{\log(2|\mathcal{F}|K/\delta)}{KM}} \\
&= 64C_{\nu,\pi} R(R+1) \sqrt{\frac{\log(2|\mathcal{F}|K/\delta)}{N}} \\
&:= \epsilon_{stat} \tag{11}
\end{aligned}$$

□

Theorem 1 (Main Theorem). *For an utterance-level MDP with discount factor γ^L , where L is the maximum length of each utterance, suppose utterance-level Assumption 1 and 2 holds, let f be the final Q function returned by Fitted Policy Evaluation formalized in Algorithm 2 at the utterance level, yields a suboptimality gap of*

$$\begin{aligned}
&\mathbb{E}_{s,a \sim d^\pi} [((\bar{f}(s,a) - \mathbb{E}_{a' \sim \pi(\cdot|s)}[\bar{f}(s,a)]) - A^\pi(s,a))^2] \\
&\leq \frac{4}{1-\gamma} (\epsilon_{stat} + 2(R+1)\sqrt{\epsilon_{stat}}) \\
&\leq \frac{4}{\gamma L(1-\gamma^{1/L})} (\epsilon_{stat} + 2(\frac{1}{1-\gamma} + 1)\sqrt{\epsilon_{stat}}).
\end{aligned}$$

For an equivalent token-level MDP with discount factor $\gamma^{1/L}$, suppose token-level Assumption 1 and 2 holds, let f be the final Q function returned by Fitted Policy Evaluation formalized in Algorithm 2 at the token level, yields a suboptimality gap of

$$\begin{aligned}
&\mathbb{E}_{s,a \sim d^\pi} [((\bar{f}(s,a) - \mathbb{E}_{a' \sim \pi(\cdot|s)}[\bar{f}(s,a)]) - \tilde{A}^\pi(s,a))^2] \\
&\leq \frac{4}{(1-\gamma^{1/L})L^{1/2}} (\epsilon_{stat} + 2(\frac{1}{1-\gamma} + 1)\sqrt{\epsilon_{stat}}L^{1/4}),
\end{aligned}$$

where ϵ_{stat} is the statistical error defined in Line 11 proportional to $N^{-1/2}$ the number of utterance-level transitions. This error term is defined the same for both utterance-level MDP and token-level MDP.

Proof. First, we start with analyzing utterance-level FPE with effective number of samples, we start

by bounding the errors of the Q functions:

$$\begin{aligned}
 & \mathbb{E}_{s,a \sim d^\pi} (\bar{f}(s, a) - Q^\pi(s, a))^2 \\
 = & \mathbb{E}_{s,a \sim d^\pi} (\bar{f}(s, a) - \mathcal{T}^\pi \bar{f}(s, a) + \mathcal{T}^\pi \bar{f}(s, a) - Q^\pi(s, a))^2 \\
 = & \mathbb{E}_{s,a \sim d^\pi} [(\bar{f}(s, a) - \mathcal{T}^\pi \bar{f}(s, a))^2 + 2(\bar{f}(s, a) - \mathcal{T}^\pi \bar{f}(s, a))(\mathcal{T}^\pi \bar{f}(s, a) - Q^\pi(s, a)) + (\mathcal{T}^\pi \bar{f}(s, a) - Q^\pi(s, a))^2] \\
 \leq & \mathbb{E}_{s,a \sim d^\pi} [(\bar{f}(s, a) - \mathcal{T}^\pi \bar{f}(s, a))^2] + 2\sqrt{\mathbb{E}_{s,a \sim d^\pi} (\bar{f}(s, a) - \mathcal{T}^\pi \bar{f}(s, a))^2 (\mathcal{T}^\pi \bar{f}(s, a) - Q^\pi(s, a))^2} \\
 & + \mathbb{E}_{s,a \sim d^\pi} [(\mathcal{T}^\pi \bar{f}(s, a) - Q^\pi(s, a))^2] \\
 \leq & \mathbb{E}_{s,a \sim d^\pi} [(\bar{f}(s, a) - \mathcal{T}^\pi \bar{f}(s, a))^2] + 2(R+1)\sqrt{\mathbb{E}_{s,a \sim d^\pi} (\bar{f}(s, a) - \mathcal{T}^\pi \bar{f}(s, a))^2} + \mathbb{E}_{s,a \sim d^\pi} [(\mathcal{T}^\pi \bar{f}(s, a) - Q^\pi(s, a))^2] \\
 \leq & \mathbb{E}_{s,a \sim d^\pi} [(\bar{f}(s, a) - \mathcal{T}^\pi \bar{f}(s, a))^2] + 2(R+1)\sqrt{\mathbb{E}_{s,a \sim d^\pi} (\bar{f}(s, a) - \mathcal{T}^\pi \bar{f}(s, a))^2} \\
 & + \gamma^2 \mathbb{E}_{s,a \sim d^\pi, s' \sim P(\cdot|s,a), a' \sim \pi(\cdot|s')} [(\bar{f}(s', a') - Q^\pi(s', a'))^2] \\
 \leq & \mathbb{E}_{s,a \sim d^\pi} [(\bar{f}(s, a) - \mathcal{T}^\pi \bar{f}(s, a))^2] + 2(R+1)\sqrt{\mathbb{E}_{s,a \sim d^\pi} (\bar{f}(s, a) - \mathcal{T}^\pi \bar{f}(s, a))^2} + \gamma \mathbb{E}_{s,a \sim d^\pi} (\bar{f}(s, a) - Q^\pi(s, a))^2,
 \end{aligned}$$

where the first inequality follows from Jensen's inequality, and the second inequality follows from $\max_{s,a} \max\{|\mathcal{T}^\pi \bar{f}(s, a)|, |Q^\pi(s, a)|\} \leq R+1$, the third inequality follows again from Jensen's inequality, and the fourth inequality follows from Lemma 5. Finally, we get:

$$\begin{aligned}
 & \mathbb{E}_{s,a \sim d^\pi} (\bar{f}(s, a) - Q^\pi(s, a))^2 \\
 \leq & \frac{1}{1-\gamma} (\mathbb{E}_{s,a \sim d^\pi} [(\bar{f}(s, a) - \mathcal{T}^\pi \bar{f}(s, a))^2] + 2(R+1)\sqrt{\mathbb{E}_{s,a \sim d^\pi} (\bar{f}(s, a) - \mathcal{T}^\pi \bar{f}(s, a))^2}) \\
 = & \frac{1}{1-\gamma} (\epsilon_{stat} + 2(R+1)\sqrt{\epsilon_{stat}}),
 \end{aligned}$$

where ϵ_{stat} is defined in Line 11. Finally, we can directly bound the errors for the advantages:

$$\begin{aligned}
 & \mathbb{E}_{s,a \sim d^\pi} [((\bar{f}(s, a) - \mathbb{E}_{a' \sim \pi(\cdot|s)} \bar{f}(s, a)) - A^\pi(s, a))^2] \\
 = & \mathbb{E}_{s,a \sim d^\pi} [((\bar{f}(s, a) - \mathbb{E}_{a' \sim \pi(\cdot|s)} \bar{f}(s, a)) - (Q^\pi(s, a) - \mathbb{E}_{a' \sim \pi(\cdot|s)} Q^\pi(s, a)))^2] \\
 \leq & 2\mathbb{E}_{s,a \sim d^\pi} [(\bar{f}(s, a) - Q^\pi(s, a))^2] + 2\mathbb{E}_{s \sim d^\pi} [(\mathbb{E}_{a' \sim \pi(\cdot|s)} [\bar{f}(s, a') - Q^\pi(s, a')])^2] \\
 \leq & 4\mathbb{E}_{s,a \sim d^\pi} [(\bar{f}(s, a) - Q^\pi(s, a))^2] \\
 \leq & \frac{4}{1-\gamma} (\epsilon_{stat} + 2(R+1)\sqrt{\epsilon_{stat}}), \\
 \leq & \frac{4}{(1-\gamma^{1/L})\gamma L} (\epsilon_{stat} + 2(R+1)\sqrt{\epsilon_{stat}}) \\
 = & \frac{4}{(1-\gamma^{1/L})\gamma L} (\epsilon_{stat} + 2(\frac{1}{1-\gamma} + 1)\sqrt{\epsilon_{stat}})
 \end{aligned}$$

where the second inequality follows from Jensen's inequality, and the fourth inequality follows from Lemma 4. A similar analysis can be done with token-level FPE, noticing that the effective number of samples for token-level FPE is NL because each utterance transition can be splitted into L token transitions:

$$\begin{aligned}
 \mathbb{E}_{s,a \sim \tilde{d}^\pi} [((\bar{f}(s, a) - \mathbb{E}_{a' \sim \pi(\cdot|s)} \bar{f}(s, a)) - \tilde{A}^\pi(s, a))^2] & \leq \frac{4}{1-\gamma} (\epsilon_{stat} L^{-1/2} + 2(R+1)\sqrt{\epsilon_{stat}} L^{-1/4}). \\
 & \leq \frac{4}{(1-\gamma)L^{1/2}} (\epsilon_{stat} + 2(\frac{1}{1-\gamma} + 1)\sqrt{\epsilon_{stat}} L^{1/4}).
 \end{aligned}$$

□

G.5. Technical Lemmas

First, we would like to prove an interesting lemma that allows us to compare the different discount factors for token level $\gamma^{1/L}$ and utterance level γ .

Lemma 4. *With the discount factor $\gamma \in (0, 1)$, and L being a positive number, we have that:*

$$\begin{aligned} \frac{1}{1-\gamma} &= \frac{1}{(1-\gamma^{1/L})(1+\gamma^{1/L}+\gamma^{2/L}+\dots+\gamma^{(L-1)/L})} \\ &\leq \frac{1}{L\gamma(1-\gamma^{1/L})} \end{aligned}$$

Below are some common technical lemmas useful for reinforcement learning.

Lemma 5 ((Zhou et al., 2023b, Lemma 2)). *For any policy π , and non-negative function $g(s, a)$, we have:*

$$\mathbb{E}_{\bar{s}, \bar{a} \sim d^\pi} \mathbb{E}_{s \sim P(\cdot | \bar{s}, \bar{a}), a \sim \pi(a|s)} [g(s, a)] \leq \frac{1}{\gamma} \mathbb{E}_{s, a \sim d^\pi} [g(s, a)].$$

where μ_0 denotes the initial state distribution (which is the same for all policies π).

Proof. Recall that $\lim_{h \rightarrow \infty} \gamma^h = 0$. We start by noting that:

$$\begin{aligned} d^\pi(s, a) &= (1-\gamma)(\mu_0(s, a) + \gamma d_1^\pi(s, a) + \gamma^2 d_2^\pi(s, a) + \dots) \tag{12} \\ &\geq \gamma(1-\gamma) \left(\sum_{\bar{s}, \bar{a}} \mu_0(\bar{s}, \bar{a}) P(s|\bar{s}, \bar{a}) \pi(a|s) + \gamma \sum_{\bar{s}, \bar{a}} d_1^\pi(\bar{s}, \bar{a}) P(s|\bar{s}, \bar{a}) \pi(a|s) + \dots \right) \\ &= \gamma(1-\gamma) \sum_{\bar{s}, \bar{a}} (\mu_0(\bar{s}, \bar{a}) + \gamma d_1^\pi(\bar{s}, \bar{a}) + \dots) P(s|\bar{s}, \bar{a}) \pi(a|s) \\ &= \gamma \sum_{\bar{s}, \bar{a}} d^\pi(\bar{s}, \bar{a}) P(s|\bar{s}, \bar{a}) \pi(a|s) \tag{13} \\ &= \gamma \mathbb{E}_{\bar{s}, \bar{a} \sim d^\pi} [P(s|\bar{s}, \bar{a}) \pi(a|s)], \end{aligned}$$

where Line 13 follows by plugging in the relation in Line 12 for \bar{s}, \bar{a} . The above implies that for any function $g \geq 0$,

$$\sum_{s, a} d^\pi(s, a) g(s, a) \geq \sum_{s, a} \gamma \mathbb{E}_{\bar{s}, \bar{a} \sim d^\pi} [P(s|\bar{s}, \bar{a}) \pi(a|s) g(s, a)],$$

which implies that

$$\mathbb{E}_{\bar{s}, \bar{a} \sim d^\pi} \mathbb{E}_{s \sim P(\cdot | \bar{s}, \bar{a}), a \sim \pi(a|s)} [g(s, a)] \leq \frac{1}{\gamma} \mathbb{E}_{s, a \sim d^\pi} [g(s, a)].$$

□

Lemma 6 (Least squares generalization bound, (Song et al., 2023, Lemma 3)). *Let $R > 0$, $\delta \in (0, 1)$, and consider a sequential function estimation setting with an instance space \mathcal{X} and target space \mathcal{Y} . Let $\mathcal{H} : \mathcal{X} \mapsto [-R, R]$ be a class of real valued functions. Let $\mathcal{D} = \{(x_1, y_1), \dots, (x_T, y_T)\}$ be a dataset of T points where $x_t \sim \rho_t := \rho_t(x_{1:t-1}, y_{1:t-1})$, and y_t is sampled via the conditional probability $p_t(x_t)$ (which could be adversarially chosen). Additionally, suppose that $\max_t |y_t| \leq R$ and $\max_h \max_x |h(x)| \leq R$. Then, the least square solution $\hat{h} \leftarrow \operatorname{argmin}_{h \in \mathcal{H}} \sum_{t=1}^T (h(x_t) - y_t)^2$ satisfies*

$$\sum_{t=1}^T \mathbb{E}_{x \sim \rho_t, y \sim p_t(x)} \left[(\hat{h}(x) - y)^2 \right] \leq 3 \inf_{h \in \mathcal{H}} \sum_{t=1}^T \mathbb{E}_{x \sim \rho_t, y \sim p_t(x)} [(h(x) - y)^2] + 256R^2 \log(2|\mathcal{H}|/\delta)$$

with probability at least $1 - \delta$.